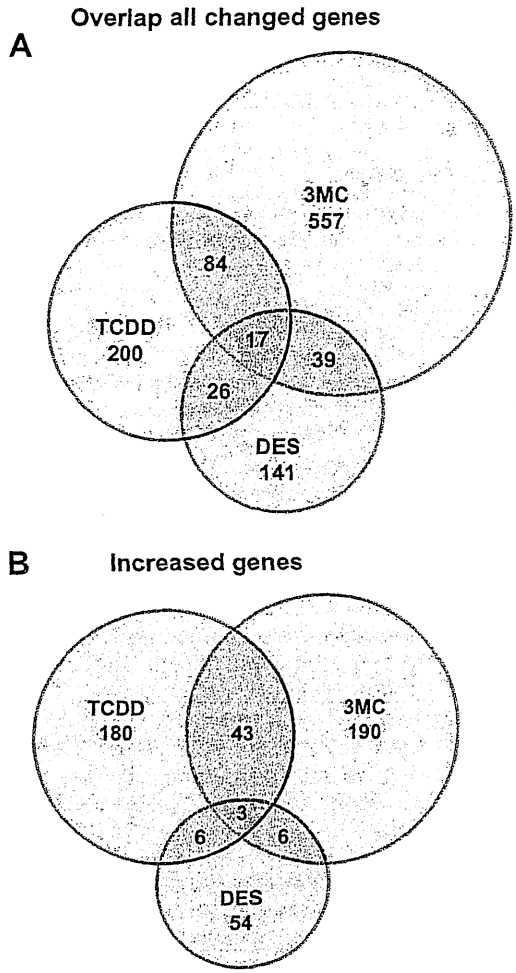

Fig. 1. Microarray data analysis. (A) Venn-diagram depicting the overlap of genes with changed expression upon treatment. (B) Venn-diagram depicting the overlap of genes with increased expression upon treatment.

700 genes with significantly altered expression, twice as many as DES and three times as many as affected by TCDD (see Fig. 1A). This is possibly an effect caused by the multitude of metabolites derived from 3-MC, and their actions within the cell.

In order to assess if the genes induced by 3-MC could be direct AhR or ER targets, we extracted the promoter sequences of the 20 genes whose expression was most up-regulated by 3-MC using the Genomatix software Gene2Promoter. These promoter sequences were analyzed by MatInspector, which retrieves conserved transcription factor binding sites. In the promoter sequences that have no published ERE or XRE sites, the program predicted either ERE or XRE or both sites in all but one (Aquaporin 3) promoter sequences (Table 1). Seven out of the 20 promoters contained one or more predicted or published ERE but no XRE. This was in contrast to the 20 genes whose expression was most up-regulated by TCDD, where only one promoter contained an ERE sequence in the absence of an XRE (data not shown). Thus, this *in silico*-based approach confirmed the presence of putative estrogen receptor binding sites in promoter regions of 3-MC regulated genes, which could suggest that 3-MC or its metabolites induce transcription of these genes by activating estrogen receptor.

The regulated genes were then classified depending on their biological function. Again, this clustering analysis showed that 3-MC and TCDD affected regulatory pathways only partly overlap (Table 2). DES and 3-MC up-regulated mostly genes that are involved in developmental processes. Additionally, genes up-regulated by DES are involved in metabolic processes while 3-MC up-regulated genes act in apoptosis and programmed cell death. In contrast, genes induced by TCDD were found mainly to be involved in nutrient transport and cellular signaling cascades. Developmental processes were only minimally affected by TCDD. Taken together, the results show three distinct chemicals having profoundly different effects in these cells.

3.2. 3-MC activates ER-target genes via ER

To validate the changes in the expression profiles identified by the microarray analysis, a set of regulated genes was chosen and analyzed using quantitative real-time PCR. We chose to use different HepG2-derived cell lines, stably transfected with either ERα (HepELN-ERα) or ERβ (HepELN-ERβ) (Riu et al., 2011). The use of these cell lines allowed us firstly, to show that the findings are not specific for HepG2-ERα cells and secondly, to assess the effects of the treatments on each estrogen receptor subtype separately. Although ERα is the predominant ER isoform in the liver, ERβ has been shown to be expressed and to exert some functions in this tissue (Barros and Gustafsson, 2011), and ERβ signaling is functioning in the HepELN-ERβ cell line (Riu et al., 2011).

HepELN-ERα cells, HepELN-ERβ cells, and the control cell line HepELN lacking ER were treated with DES, 3-MC or TCDD and mRNA levels were determined by quantitative RT-PCR. We chose two exposure times: one similar to the one used for the microarray study (20 h) and a shorter one (6 h). The latter was chosen to test whether the chemicals regulate the investigated genes directly or indirectly by controlling genes upstream of the investigated ones.

For the analysis, we chose the known ER target gene TFF1/pS2, insulin-like growth factor binding protein 4 (IFBP4), also a known ER target gene (Bourdeau et al., 2004; Denger et al., 2008) and the most highly DES-induced gene not induced by 3-MC, plasminogen activator inhibitor-1/Serpine I (PAI-1), which was the most highly 3-MC-induced gene not induced by DES, and follistatin (FST), which was among the top 20 induced by both DES and 3-MC.

As expected, the estrogen DES induced transcription of both known ER-target genes via ERα at both time points (Fig. 2A and B). Induction of transcription via ERβ was less pronounced and only measured after 20 h of treatment. 3-MC induced TFF1/pS2 at both time points, whereas for IGFBP4 induction was only measured at the 6 h time point. Interestingly, 3-MC could induce the two genes only via ERα, whereas no effect via ERβ was observed. TCDD treatment had no effect on the transcription of these two genes.

PAI-1 could be induced by 3-MC at both time points, but again only in ERα-expressing cells (Fig. 2C). The effect of DES was slightly less pronounced and only measurable after 6 h, not after 20 h. The short effect of DES on PAI-1 and of 3-MC on IGFBP4 could explain the discrepancies to the microarray results as the cells were treated for 24 h for the microarray analysis. FST was induced by both compounds, however, only treatment of DES led to increased expression in the ERβ-expressing cells (Fig. 2D).

To conclude, we have identified ER-activated regulation of TFF1/pS2, PAI-1, and FST by the polycyclic aromatic hydrocarbon 3-MC, or by a metabolite of the parent compound. The estrogenic activities exerted by 3-MC, or its derivative, seem to be mediated exclusively by ERα, which suggests an ER isoform-selectivity of the active compound.

3.3. 3-MC induces recruitment of ERα to target gene promoters

Our results so far suggest that 3-MC, or rather a metabolite of this compound, displays estrogenic activities that are dependent

Table 2
Gene ontology (GO) of the genes upregulated by DES, 3-MC, and TCDD.

Term	ID	Total	Observed	Expected	ZScore
Genes up-regulated by DES					
Multicellular organismal process	GO:0032501	2983	23	11.17	3.92
Organ development	GO:0048513	1127	11	4.22	3.43
Cell proliferation	GO:0008283	748	8	2.8	3.19
System development	GO:0048731	1555	13	5.82	3.13
Organ morphogenesis	GO:0009887	369	5	1.38	3.12
Multicellular organismal development	GO:0007275	2113	16	7.91	3.08
Anatomical structure development	GO:0048856	1792	14	6.71	2.99
Carbohydrate metabolic process	GO:0005975	389	5	1.46	2.98
Developmental process	GO:0032502	2925	19	10.95	2.68
Phosphorus metabolic process	GO:0006793	888	8	3.33	2.64
Phosphate metabolic process	GO:0006796	888	8	3.33	2.64
Phosphorylation	GO:0016310	741	7	2.77	2.6
Genes up-regulated by 3-MC					
Regulation of developmental process	GO:0050793	786	18	3.66	7.71
Organ development	GO:0048513	1127	19	5.24	6.24
Developmental process	GO:0032502	2925	34	13.6	6.11
Positive regulation of biological process	GO:0048518	1111	18	5.17	5.86
Regulation of cell differentiation	GO:0045595	176	6	0.82	5.77
Apoptosis	GO:0006915	761	14	3.54	5.71
Negative regulation of transcription from RNA polymerase II promoter	GO:0000122	130	5	0.6	5.69
Programmed cell death	GO:0012501	769	14	3.58	5.66
Epidermis development	GO:0008544	133	5	0.62	5.61
Regulation of phosphorylation	GO:0042325	89	4	0.41	5.6
Cell death	GO:0008219	816	14	3.79	5.39
Death	GO:0016265	816	14	3.79	5.39
Genes up-regulated by TCDD					
Carboxylic acid transport	GO:0046942	79	5	0.38	7.51
Amino acid transport	GO:0006865	56	4	0.27	7.2
Amine transport	GO:0015837	71	4	0.34	6.27
G-protein signaling, coupled to cyclic nucleotide second messenger	GO:0007187	88	4	0.43	5.51
Cyclic-nucleotide-mediated signaling	GO:0019935	95	4	0.46	5.25
Positive regulation of biological process	GO:0048518	1111	16	5.37	4.76
Positive regulation of cellular process	GO:0048522	1008	14	4.87	4.28
Negative regulation of transcription from RNA polymerase II promoter	GO:0000122	130	4	0.63	4.28
Sensory perception of sound	GO:0007605	134	4	0.65	4.19
Anatomical structure development	GO:0048856	1792	20	8.66	4.09
System development	GO:0048731	1555	18	7.51	4.03
Nervous system development	GO:0007399	673	10	3.25	3.83

The GO analysis was carried out using BiblioSphere (Genomatix).

on ERα. To further corroborate a mechanism involving ERα activation, we analyzed ERα recruitment upon 3-MC and DES treatment to IGFBP4, FST, and GREB1 as positive control. To this end, we performed chromatin immunoprecipitations assays (ChIPs) in HepELN-ERα cells. ER recruitment to target promoters is usually seen very shortly after ligand treatment, thus incubation times between 15 and 45 min are normally used in ChIP protocols. We assumed that such a short incubation time would not allow for sufficient accumulation of 3-MC metabolites, thus we treated the cells for 2 h with DES, 3-MC, and TCDD. Precipitations were performed with antibodies against ERα, AhR and ARNT. The precipitated DNA was analyzed by real-time PCR amplifying either known functional EREs (GREB1 promoter (Ruegg et al., 2008), IGFBP4 enhancer (Bourdeau et al., 2004; Denger et al., 2008)) or an ERE in the FST promoter identified by *in silico* analysis (Fig. 3B).

In line with the expression data, the ChIP results show recruitment of ERα to these regions upon treatment with DES or 3-MC, but not with TCDD (Fig. 3A–C). Neither AhR nor ARNT was recruited, suggesting that 3-MC acts via ERα.

In control experiments, a xenobiotic response element (XRE) in the promoter region of the CYP1A1 gene was analyzed in the same cells, and ERα was not found to associate to this region (Fig. 3D). When precipitations were carried out with AhR or ARNT antibodies, we found high enrichment of both AhR and ARNT at the CYP1A1 enhancer in the presence of both 3-MC and TCDD, confirming our treatments and the responsiveness of the cell model.

These findings demonstrate that 3-MC, just like DES, can induce ERα-recruitment to EREs in target genes, independently of ARNT- or AhR-recruitment. This is true not only for known ERα-target genes (like GREB-1 and IGFBP4) but also for FST, identifying FST as a novel ER-target gene.

4. Discussion

TCDD and 3-MC are widely used as prototypical AhR ligands and CYP1A1 inducers, however, their precise biological response patterns have not been characterized. In this study, we compared the transcriptional response to TCDD, 3-MC and DES in HepG2 cells, a cell line that is able to metabolize 3-MC. The microarray analysis showed that, while 24 h treatment with DES and TCDD affected around 200 and 300 genes, respectively, 3-MC treatment significantly altered the expression of almost 700 genes. We suggest that this outcome reflects the high number of metabolites generated by biotransformation of 3-MC in HepG2 cells, and their actions within the cell.

Importantly, 3-MC and TCDD control distinct gene networks and biological functions. 3-MC has frequently been used as an AhR agonist instead of TCDD in both *in vitro* and *in vivo* studies, due to strict national regulations controlling the use of dioxin in laboratories. The findings presented here clearly show that data obtained with 3-MC cannot be generalized for other AhR ligands, particularly not for TCDD.

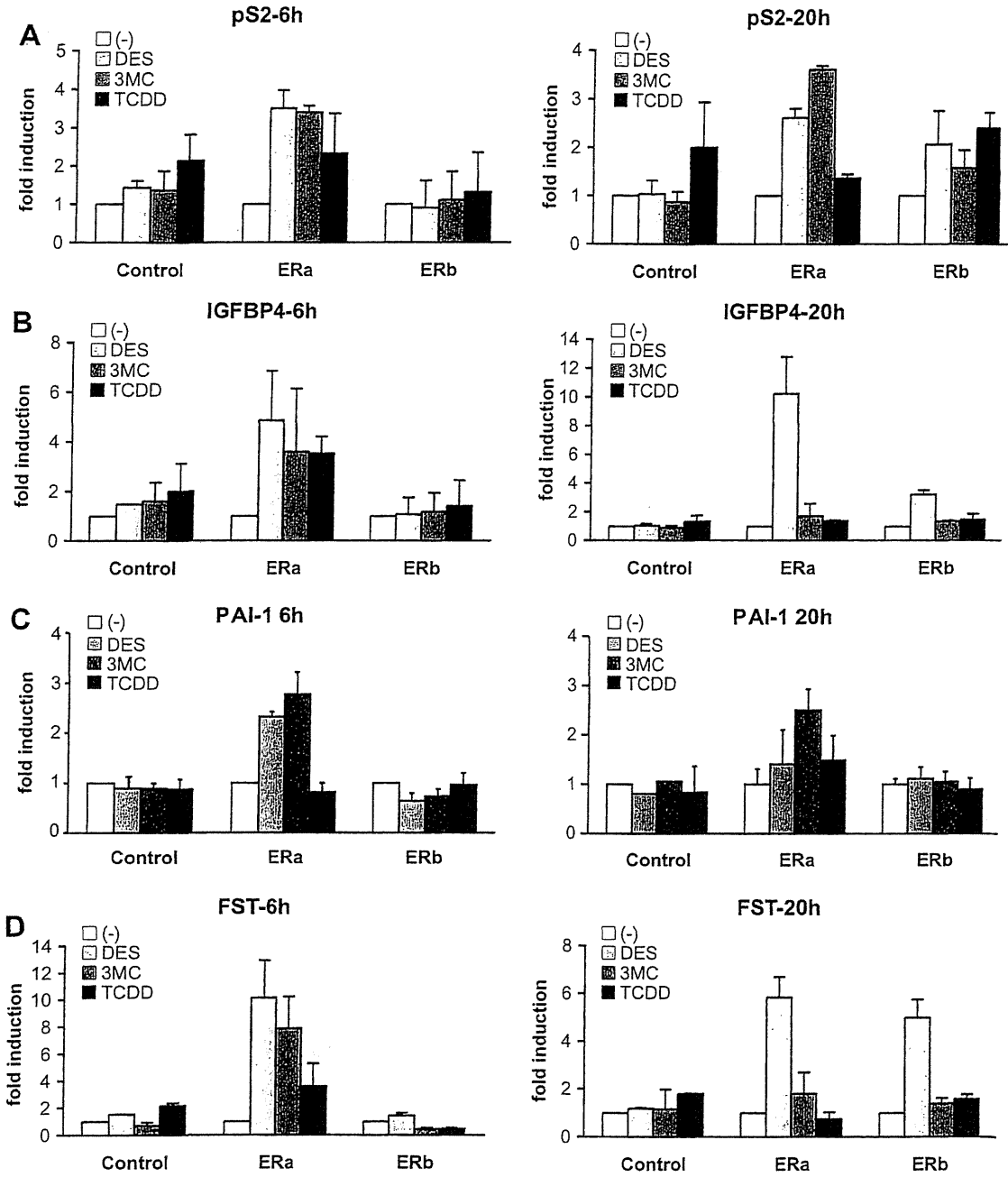

Fig. 2. Validation of microarray data (qRT-PCR). Verification of the microarray data was carried out as described in Materials and methods. Total RNA from control HepELN, HepELN-ERα or HepELN-ERβ cells treated with DES-, 3-MC or TCDD was prepared after 6 h and 20 h. The relative level of mRNA of regulated genes was then analyzed by quantitative RT-PCR. Samples were analyzed in triplicates and are given as SEM. (A) TFF1/pS2; (B) IGFBP-4; (C) PAI-1; (D) FST.

Endocrine disruption has been extensively documented, in particular for the estrogen receptor. TCDD and 3-MC have both been shown to interfere with the ERs but by different mechanisms of action. We and others could demonstrate that 3-MC, or rather some of its metabolites, act as ERα ligands (Abdelrahim et al., 2006; Swedenborg et al., 2008). TCDD, on the other hand, inhibits ER-mediated gene transcription by indirect mechanisms, e.g. by inducing competition between ER and AhR for their common co-activator ARNT (Brunnberg et al., 2003; Ruegg et al., 2008; Safe et al., 2000). In this study, we could confirm that 3-MC can induce ER-target genes in an ERα-dependent manner. The induction was apparent already after 6 h of treatment, suggesting that 3-MC derived compounds act directly on ERα. This notion was corroborated by the finding that ERα is recruited to predicted ERE sequences located in the target gene promoters upon 3-MC treatment. A complex molecular interplay between the AhR and ER can occur on some promoters (Klinge et al., 2000; Matthews et al., 2005; Safe and McDougal, 2002; Safe et al., 2000; Spink et al., 2003; Wang et al., 2001; Wormke et al., 2000; Zacharewski et al., 1994). However, on the promoters analyzed in this study, no co-recruitment of ERα, AhR, and ARNT could be measured.

Intriguingly, the estrogenic effect of 3-MC was only detected in ERα-expressing cells but not in ERβ-expressing cells. This result indicates that, in contrast to DES, the active 3-MC metabolite acts through an isoform-selective mechanism. Again, this is in contrast to TCDD that has been shown to interfere in particular with ERβ (Ruegg et al., 2008).

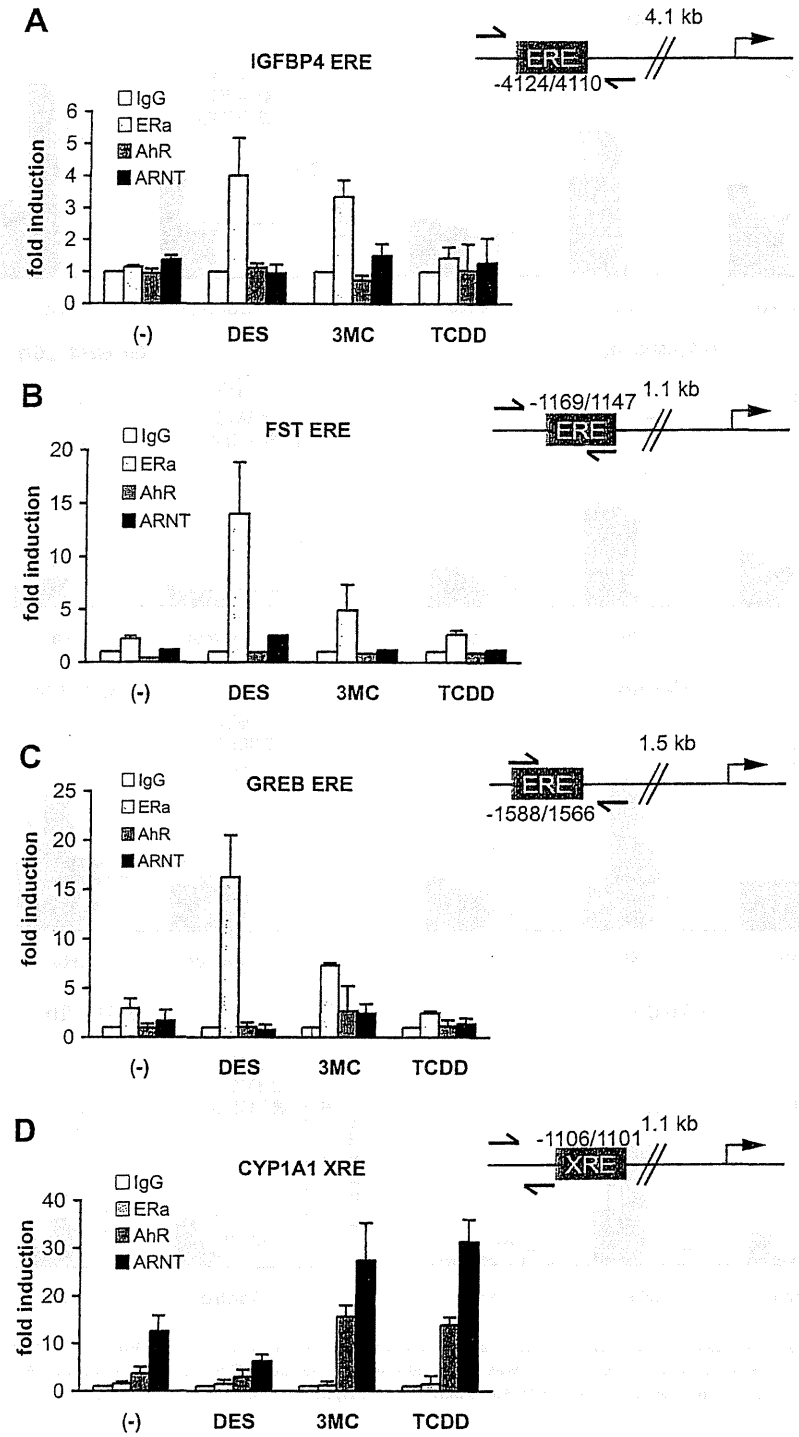

Fig. 3. Chromatin immunoprecipitations (ChIPs). HepELN-ERα cells were treated for 2 h as described in Materials and methods. ChIPs were carried out with antibodies directed against ERα, AhR and ARNT. Enrichment to regulatory regions comprising EREs or an XRE was analyzed with quantitative real-time PCR. (A) IGFBP4 (ERE – 4.1 kb); (B) FST (ERE – 1.1 kb); (C) GREB-1 (ERE – 1.5 kb); (D) CYP1A1 (XRE – 1.1 kb).

In addition to the known ER target genes, DES and 3-MC induced genes that have not been shown previously to be regulated by ER. For FST and PAI-1 we could confirm that they are regulated by activated ERα, FST also by activated ERβ. As their expression was already upregulated after 6 h we speculated that they are novel direct ER target genes. Indeed, we could identify potential ER binding sites in the promoter region of these genes. For FST, we could show DES and 3-MC-dependent ERα-recruitment to a predicted ERE, confirming it to be a direct ERα-target gene. FST is important for the development of bone, muscle, and skin (Matzuk et al., 1995), and is essential for functioning of the female and male gonads (reviewed in e.g. de Kretser et al., 2002). Our finding that 3-MC can induce FST-expression calls for further experiments evaluating the effects of 3-MC on FST in these systems.

5. Conclusions

We have shown that the prototypical AhR ligands TCDD and 3-MC control separate gene regulatory networks and have distinct impacts on the cells. Thus care should be taken when interpreting

studies that use these two compounds interchangeably. In contrast to TCDD, 3-MC induces known estrogen-responsive genes such as GREB1, IGFBP4 and TFF1/pS2 as well as genes not previously reported to be ER target genes, like FST and PAI-1/Serpine1. Furthermore, estrogenicity of 3-MC, or some of its metabolites, is ER isoform-selective, affecting only ERα.

Acknowledgement

We are grateful to Patrick Balaguer, INSERM, Montpellier, France for providing the HepELN cell lines used in this study.

Appendix A. Supplementary data

Supplementary data associated with this article can be found, in the online version, at http://dx.doi.org/10.1016/j.mce.2012.05.006.

References

Abdelrahim, M., Ariazi, E., Kim, K., Khan, S., Barhoumi, R., Burghardt, R., Liu, S., Hill, D., Finnell, R., Wlodarczyk, B., Jordan, V.C., Safe, S., 2006. 3-Methylcholanthrene and other aryl hydrocarbon receptor agonists directly activate estrogen receptor alpha. Cancer Res. 66, 2459–2467.

Abdelrahim, M., Smith 3rd, R., Safe, S., 2003. Aryl hydrocarbon receptor gene silencing with small inhibitory RNA differentially modulates Ah-responsiveness in MCF-7 and HepG2 cancer cells. Mol. Pharmacol. 63, 1373–1381.

Astroff, B., Safe, S., 1990. 2,3,7,8-Tetrachlorodibenzo-p-dioxin as an antiestrogen: effect on rat uterine peroxidase activity. Biochem. Pharmacol. 39, 485–488.

Barkhem, T., Andersson-Ross, C., Hoglund, M., Nilsson, S., 1997. Characterization of the "estrogenicity" of tamoxifen and raloxifene in HepG2 cells: regulation of gene expression from an ERE controlled reporter vector versus regulation of the endogenous SHBG and PS2 genes. J. Steroid Biochem. Mol. Biol. 62, 53–64.

Barros, R.P., Gustafsson, J.A., 2011. Estrogen receptors and the metabolic network. Cell Metab. 14, 289–299.

Bourdeau, V., Deschenes, J., Metivier, R., Nagai, Y., Nguyen, D., Bretschneider, N., Gannon, F., White, J.H., Mader, S., 2004. Genome-wide identification of high-affinity estrogen response elements in human and mouse. Mol. Endocrinol. 18, 1411–1427.

Boverhof, D.R., Burgoon, L.D., Williams, K.J., Zacharewski, T.R., 2008. Inhibition of estrogen-mediated uterine gene expression responses by dioxin. Mol. Pharmacol. 73, 82–93.

Brunnberg, S., Pettersson, K., Rydin, E., Matthews, J., Hanberg, A., Pongratz, I., 2003. The basic helix-loop-helix-PAS protein ARNT functions as a potent coactivator of estrogen receptor-dependent transcription. Proc. Natl. Acad Sci. USA 100, 6517–6522.

Burchiel, S.W., Thompson, T.A., Lauer, F.T., Oprea, T.I., 2007. Activation of dioxin response element (DRE)-associated genes by benzo(a)pyrene 3,6-quinone and benzo(a)pyrene 1,6-quinone in MCF-10A human mammary epithelial cells. Toxicol. Appl. Pharmacol. 221, 203–214.

Burdette, J.E., Woodruff, T.K., 2007. Activin and estrogen crosstalk regulates transcription in human breast cancer cells. Endocr. Relat. Cancer 14, 679–689.

Bursztyka, J., Perdu, E., Pettersson, K., Pongratz, I., Fernandez-Cabrera, M., Olea, N., Debrauwer, L., Zalko, D., Cravedi, J.P., 2008. Biotransformation of genistein and bisphenol A in cell lines used for screening endocrine disruptors. Toxicol. In Vitro 22, 1595–1604.

Chaloupka, K., Krishnan, V., Safe, S., 1992. Polynuclear aromatic hydrocarbon carcinogens as antiestrogens in MCF-7 human breast cancer cells: role of the Ah receptor. Carcinogenesis 13, 2233–2239.

Charles, G.D., Bartels, M.J., Zacharewski, T.R., Gollapudi, B.B., Freshour, N.L., Carney, E.W., 2000. Activity of benzo[a]pyrene and its hydroxylated metabolites in an estrogen receptor-alpha reporter gene assay. Toxicol. Sci. 55, 320–326.

de Kretser, D.M., Hedger, M.P., Loveland, K.L., Phillips, D.J., 2002. Inhibins, activins and follistatin in reproduction. Hum. Reprod. Update 8, 529–541.

Denger, S., Bahr-Ivacevic, T., Brand, H., Reid, G., Blake, J., Seifert, M., Lin, C.Y., May, K., Benes, V., Liu, E.T., Gannon, F., 2008. Transcriptome profiling of estrogen-regulated genes in human primary osteoblasts reveals an osteoblast-specific regulation of the insulin-like growth factor binding protein 4 gene. Mol. Endocrinol. 22, 361–379.

Elobeid, M.A., Allison, D.B., 2008. Putative environmental-endocrine disruptors and obesity: a review. Curr. Opin. Endocrinol. Diabetes Obes. 15, 403–408.

Gozgit, J.M., Nestor, K.M., Fasco, M.J., Pentecost, B.T., Arcaro, K.F., 2004. Differential action of polycyclic aromatic hydrocarbons on endogenous estrogen-responsive genes and on a transfected estrogen-responsive reporter in MCF-7 cells. Toxicol. Appl. Pharmacol. 196, 58–67.

Harper, N., Wang, X., Liu, H., Safe, S., 1994. Inhibition of estrogen-induced progesterone receptor in MCF-7 human breast cancer cells by aryl hydrocarbon (Ah) receptor agonists. Mol. Cell Endocrinol. 104, 47–55.

Huang, G., Elferink, C.J., 2011. A novel non-consensus xenobiotic response element capable of mediating aryl hydrocarbon receptor dependent gene expression. Mol. Pharmacol.

Iseki, M., Ikuta, T., Kobayashi, T., Kawajiri, K., 2005. Growth suppression of Leydig TM3 cells mediated by aryl hydrocarbon receptor. Biochem. Biophys. Res. Commun. 331, 902–908.

Kanno, J., Aisaki, K., Igarashi, K., Nakatsu, N., Ono, A., Kodama, Y., Nagao, T., 2006. "Per cell" normalization method for mRNA measurement by quantitative PCR and microarrays. BMC Genom. 7, 64.

Kharat, I., Saatcioglu, F., 1996. Antiestrogenic effects of 2,3,7,8-tetrachlorodibenzo-p-dioxin are mediated by direct transcriptional interference with the liganded estrogen receptor. Cross-talk between aryl hydrocarbon- and estrogen-mediated signaling. J. Biol. Chem. 271, 10533–10537.

Klinge, C.M., Kaur, K., Swanson, H.I., 2000. The aryl hydrocarbon receptor interacts with estrogen receptor alpha and orphan receptors COUP-TFI and ERRalpha1. Arch. Biochem. Biophys. 373, 163–174.

Liu, S., Abdelrahim, M., Khan, S., Ariazi, E., Jordan, V.C., Safe, S., 2006. Aryl hydrocarbon receptor agonists directly activate estrogen receptor alpha in MCF-7 breast cancer cells. Biol. Chem. 387, 1209–1213.

Mandal, S., Davie, J.R., 2010. Estrogen regulated expression of the p21 Waf1/Cip1 gene in estrogen receptor positive human breast cancer cells. J. Cell Physiol. 224, 28–32.

Matthews, J., Wihlen, B., Thomsen, J., Gustafsson, J.A., 2005. Aryl hydrocarbon receptor-mediated transcription: ligand-dependent recruitment of estrogen receptor alpha to 2,3,7,8-tetrachlorodibenzo-p-dioxin-responsive promoters. Mol. Cell Biol. 25, 5317–5328.

Matzuk, M.M., Lu, N., Vogel, H., Sellheyer, K., Roop, D.R., Bradley, A., 1995. Multiple defects and perinatal death in mice deficient in follistatin. Nature 374, 360–363.

Metivier, R., Penot, G., Hubner, M.R., Reid, G., Brand, H., Kos, M., Gannon, F., 2003. Estrogen receptor-alpha directs ordered, cyclical, and combinatorial recruitment of cofactors on a natural target promoter. Cell 115, 751–763.

Moller, F.J., Diel, P., Zierau, O., Hertrampf, T., Maass, J., Vollmer, G., 2010. Long-term dietary isoflavone exposure enhances estrogen sensitivity of rat uterine responsiveness mediated through estrogen receptor alpha. Toxicol. Lett. 196, 142–153.

Mukherjee, S., Koner, B.C., Ray, S., Ray, A., 2006. Environmental contaminants in pathogenesis of breast cancer. Indian J. Exp. Biol. 44, 597–617.

Newbold, R.R., Padilla-Banks, E., Jefferson, W.N., Heindel, J.J., 2008. Effects of endocrine disruptors on obesity. Int. J. Androl. 31, 201–208.

Nilsson, S., Makela, S., Treuter, E., Tujague, M., Thomsen, J., Andersson, G., Enmark, E., Pettersson, K., Warner, M., Gustafsson, J.A., 2001. Mechanisms of estrogen action. Physiol. Rev. 81, 1535–1565.

Nomura, T., 2008. Transgenerational effects from exposure to environmental toxic substances. Mutat. Res. 659, 185–193.

Pang, P.H., Lin, Y.H., Lee, Y.H., Hou, H.H., Hsu, S.P., Juan, S.H., 2008. Molecular mechanisms of p21 and p27 induction by 3-methylcholanthrene, an aryl-hydrocarbon receptor agonist, involved in antiproliferation of human umbilical vascular endothelial cells. J. Cell Physiol. 215, 161–171.

Pathak, S., D'Souza, R., Ankolkar, M., Gaonkar, R., Balasinor, N.H., 2010. Potential role of estrogen in regulation of the insulin-like growth factor2-H19 locus in the rat testis. Mol. Cell Endocrinol. 314, 110–117.

Poland, A., Knutson, J.C., 1982. 2,3,7,8-Tetrachlorodibenzo-p-dioxin and related halogenated aromatic hydrocarbons: examination of the mechanism of toxicity. Annu. Rev. Pharmacol. Toxicol. 22, 517–554.

Puga, A., Barnes, S.J., Chang, C., Zhu, H., Nephew, K.P., Khan, S.A., Shertzer, H.G., 2000. Activation of transcription factors activator protein-1 and nuclear factor-kappaB by 2,3,7,8-tetrachlorodibenzo-p-dioxin. Biochem. Pharmacol. 59, 997–1005.

Riu, A., Grimaldi, M., le Maire, A., Bey, G., Phillips, K., Boulahtouf, A., Perdu, E., Zalko, D., Bourguet, W., Balaguer, P., 2011. Peroxisome proliferator-activated receptor gamma is a target for halogenated analogs of bisphenol A. Environ. Health Perspect. 119, 1227–1232.

Ruegg, J., Penttinen-Damdimopoulou, P., Makela, S., Pongratz, I., Gustafsson, J.A., 2009. Receptors mediating toxicity and their involvement in endocrine disruption. EXS 99, 289–323.

Ruegg, J., Swedenborg, E., Wahlstrom, D., Escande, A., Balaguer, P., Pettersson, K., Pongratz, I., 2008. The transcription factor aryl hydrocarbon receptor nuclear translocator functions as an estrogen receptor beta-selective coactivator, and its recruitment to alternative pathways mediates antiestrogenic effects of dioxin. Mol. Endocrinol. 22, 304–316.

Safe, S., McDougal, A., 2002. Mechanism of action and development of selective aryl hydrocarbon receptor modulators for treatment of hormone-dependent cancers (review). Int. J. Oncol. 20, 1123–1128.

Safe, S., Wormke, M., 2003. Inhibitory aryl hydrocarbon receptor–estrogen receptor alpha cross-talk and mechanisms of action. Chem. Res. Toxicol. 16, 807–816.

Safe, S., Wormke, M., Samudio, I., 2000. Mechanisms of inhibitory aryl hydrocarbon receptor-estrogen receptor crosstalk in human breast cancer cells. J. Mammary Gland Biol. Neoplasia 5, 295–306.

Sladek, N.E., 2003. Transient induction of increased aldehyde dehydrogenase 3A1 levels in cultured human breast (adeno)carcinoma cell lines via 5′-upstream xenobiotic, and electrophile, responsive elements is, respectively, estrogen receptor-dependent and -independent. Chem. Biol. Interact. 143–144, 63–74.

Spink, D.C., Katz, B.H., Hussain, M.M., Pentecost, B.T., Cao, Z., Spink, B.C., 2003. Estrogen regulates Ah responsiveness in MCF-7 breast cancer cells. Carcinogenesis 24, 1941–1950.

Swedenborg, E., Ruegg, J., Hillenweck, A., Rehnmark, S., Faulds, M.H., Zalko, D., Pongratz, I., Pettersson, K., 2008. 3-Methylcholanthrene displays dual effects on estrogen receptor (ER) alpha and ER beta signaling in a cell-type specific fashion. Mol. Pharmacol. 73, 575–586.

Swedenborg, E., Ruegg, J., Makela, S., Pongratz, I., 2009. Endocrine disruptive chemicals: mechanisms of action and involvement in metabolic disorders. J. Mol. Endocrinol.

Szabo, P.E., Pfeifer, G.P., Mann, J.R., 2004. Parent-of-origin-specific binding of nuclear hormone receptor complexes in the H19-Igf2 imprinting control region, Mol. Cell Biol. 24, 4858–4868.

Thomas, T.J., Faaland, C.A., Adhikarakunnathu, S., Watkins, L.F., Thomas, T., 1998. Induction of p21 (CIP1/WAF1/SID1) by estradiol in a breast epithelial cell line transfected with the recombinant estrogen receptor gene: a possible mechanism for a negative regulatory role of estradiol. Breast Cancer Res. Treat. 47, 181–193.

Vasiliou, V., Reuter, S.F., Williams, S., Puga, A., Nebert, D.W., 1999. Mouse cytosolic class 3 aldehyde dehydrogenase (Aldh3a1): gene structure and regulation of constitutive and dioxin-inducible expression. Pharmacogenetics 9, 569–580.

Vidaeff, A.C., Sever, L.E., 2005. In utero exposure to environmental estrogens and male reproductive health: a systematic review of biological and epidemiologic evidence. Reprod. Toxicol. 20, 5–20.

Wang, F., Samudio, I., Safe, S., 2001. Transcriptional activation of cathepsin D gene expression by 17beta-estradiol: mechanism of aryl hydrocarbon receptor-mediated inhibition. Mol. Cell Endocrinol. 172, 91–103.

Whitlock Jr., J.P., 1999. Induction of cytochrome P4501A1. Annu. Rev. Pharmacol. Toxicol. 39, 103–125.

Wood, A.W., Chang, R.L., Levin, W., Thomas, P.E., Ryan, D., Stoming, T.A., Thakker, D.R., Jerina, D.M., Conney, A.H., 1978. Metabolic activation of 3-methylcholanthrene and its metabolites to products mutagenic to bacterial and mammalian cells. Cancer Res. 38, 3398–3404.

Wormke, M., Castro-Rivera, E., Chen, I., Safe, S., 2000. Estrogen and aryl hydrocarbon receptor expression and crosstalk in human Ishikawa endometrial cancer cells. J. Steroid Biochem. Mol. Biol. 72, 197–207.

Zacharewski, T.R., Bondy, K.L., McDonell, P., Wu, Z.F., 1994. Antiestrogenic effect of 2,3,7,8-tetrachlorodibenzo-p-dioxin on 17 beta-estradiol-induced pS2 expression. Cancer Res. 54, 2707–2713.

Reproductive Toxicology 34 (2012) 93–100

Contents lists available at SciVerse ScienceDirect

Reproductive Toxicology

journal homepage: www.elsevier.com/locate/reprotox

Increased cellular distribution of vimentin and Ret in the cingulum induced by developmental hypothyroidism in rat offspring maternally exposed to anti-thyroid agents

Hitoshi Fujimoto[a], Gye-Hyeong Woo[a], Kaoru Inoue[a], Katsuhide Igarashi[b], Jun Kanno[b], Masao Hirose[c], Akiyoshi Nishikawa[d], Makoto Shibutani[a,e,*]

[a] Division of Pathology, National Institute of Health Sciences, 1–18–1 Kamiyoga, Setagaya-ku, Tokyo 158-8501, Japan
[b] Division of Molecular Toxicology, National Institute of Health Sciences, 1–18–1 Kamiyoga, Setagaya-ku, Tokyo 158-8501, Japan
[d] Biological Safety Research Center, National Institute of Health Sciences, 1–18–1 Kamiyoga, Setagaya-ku, Tokyo 158-8501, Japan
[c] Food Safety Commission, 5–2–20 Akasaka Park Bld. 22nd Floor, Akasaka, Minato-ku, Tokyo 107-6122, Japan
[e] Laboratory of Veterinary Pathology, Tokyo University of Agriculture and Technology, 3–5–8 Saiwai-cho, Fuchu-shi, Tokyo 183-8509, Japan

ARTICLE INFO

Article history:
Received 4 December 2011
Received in revised form 19 February 2012
Accepted 16 March 2012
Available online 6 April 2012

Keywords:
Developmental hypothyroidism
Cerebral white matter
Vimentin
Ret
Rat

ABSTRACT

To elucidate target molecules of white matter development responding to hypothyroidism, global gene expression profiling of cerebral white matter from male rat offspring was performed after maternal exposure to anti-thyroid agents, 6-propyl-2-thiouracil and methimazole, on postnatal day 20. Genes involved in central nervous system development commonly up- or down-regulated among groups treated with anti-thyroid agents. Immunohistochemical distributions of vimentin, Ret proto-oncogene (Ret), deleted in colorectal cancer protein (DCC), and Claudin11 (Cld11) were examined based on the gene expression profile. Immunoreactive cells for vimentin and Ret in the cingulum, and the immunoreactive intensity of Cld11 and DCC in whole white matter were increased by treatment with anti-thyroid agents. Immunoreactive cells for vimentin and Ret were immature astrocytes and oligodendrocytes, respectively. Thus, immunoreactive cells for vimentin and Ret may be quantitatively measurable targets of developmental hypothyroidism in white matter.

1. Introduction

Thyroid hormones are essential for normal fetal and neonatal brain development, control neuronal and glial proliferation in definitive brain regions and regulate neuronal migration and differentiation [1–3]. In humans, maternal hypothyroxinemia early in pregnancy may adversely affect fetal brain development, and importantly, even mild to moderate hypothyroxinemia may result in suboptimal neurodevelopment [4], thereby increasing the concern of impaired brain development induced by exposure to thyroid hormone-disrupting chemicals in the environment.

Developmental hypothyroidism leads to growth retardation, neurological defects and impaired performance in various behavioral learning actions [5,6]. Rat offspring maternally exposed to anti-thyroid agents, such as 6-propyl-2-thiouracil (PTU) and methimazole (MMI), show impaired brain growth including white matter hypoplasia with decreased axonal myelination and oligodendrocytes, and impairment of neurogenesis, neuronal migration, dendritic arborization and synapse formation [2,7–9]. These types of impaired brain growth are permanent and accompanied by apparent structural and functional abnormalities. However, the molecular mechanism of impaired brain growth is still unclear.

Histological lesion-specific gene expression profiling provides valuable information on the mechanisms underlying lesion development. In previous studies, we established molecular analysis methods for DNA, RNA and proteins in paraffin-embedded small tissue specimens using the organic solvent-based fixative methacarn, with high performance similar to that of unfixed frozen tissue specimens [10–12]. These methods have been used to analyze global gene expression changes in microdissected lesions [13–15].

Abbreviations: CC, corpus callosum; Cld11, claudin 11; CNS, central nervous system; DCC, deleted in colorectal cancer protein; GAPDH, glyceraldehyde 3-phosphate dehydrogenase; GD, gestation day; GDNF, glial cell line-derived neurotrophic factor; GFAP, glial fibrillary acidic protein; MMI, methimazole; OSP, oligodendrocyte specific protein; PCR, polymerase chain reaction; PND, postnatal day; PTU, 6-propyl-2-thiouracil; Ret, Ret proto-oncogene; RT, reverse transcription; v-Maf, v-maf musculoaponeurotic fibrosarcoma oncogene; Zfhx1b, zinc finger homeobox 1b.

* Corresponding author at: Laboratory of Veterinary Pathology, Tokyo University of Agriculture and Technology, 3–5–8 Saiwai-cho, Fuchu-shi, Tokyo 183-8509, Japan. Tel.: +81 42 367 5874; fax: +81 42 367 5771.
E-mail address: mshibuta@cc.tuat.ac.jp (M. Shibutani).

0890-6238/$ – see front matter © 2012 Elsevier Inc. All rights reserved.
http://dx.doi.org/10.1016/j.reprotox.2012.03.005

To evaluate in vivo developmental brain growth effects of thyroid hormone-disrupting chemicals, we morphometrically analyzed neuronal migration and white matter development in a rat developmental hypothyroidism model [16]. Molecules involved in aberrant neurogenesis and neuronal mismigration were identified by global gene expression analysis of the hippocampal area [15]. In the present study, to elucidate marker molecules in white matter involved in developmental hypothyroidism, we performed global gene expression profiling using microarrays. To obtain the white matter-specific gene expression profile, a microdissection technique was applied to the corpus callosum (CC) and bilateral cerebral white matter. Based on expression profiles, cellular localization of selected molecules was then immunohistochemically examined in cerebral white matter after developmental exposure to anti-thyroid agents.

2. Materials and methods

2.1. Chemicals and animals

6-propyl-2-thiouracil (PTU; CAS No. 51-52-9) and methimazole (MMI; CAS No. 60-56-0) were purchased from Sigma Chemical Co. (St. Louis, MO). Pregnant CD® (SD) IGS rats at gestational day (GD) 3 (GD 0: the day vaginal plugs appeared) were purchased from Charles River Japan Inc. (Yokohama, Japan). Animals were individually housed in polycarbonate cages (SK-Clean, 41.5 cm × 26 cm × 17.5 cm; CLEA Japan Inc., Tokyo, Japan) with wood chip bedding (Sankyo Lab Service Corp., Tokyo, Japan) and maintained in a climate-controlled animal room (24 ± 1 °C, relative humidity: 55 ± 5%) with a 12 h light/dark cycle. A soy-free diet (Oriental Yeast Co. Ltd., Tokyo, Japan) was chosen as the basal diet for maternal animals to eliminate possible phytoestrogen effects [17]. Animals received food and water ad libitum throughout experimentation including a 1 week acclimation period.

2.2. Experimental design

Animal experiments are described elsewhere [16]. Briefly, maternal animals were randomly divided into four groups including an untreated control. Eight dams per group were treated with 3 or 12 ppm PTU or 200 ppm MMI, which was added to drinking water from GD 10 to postnatal day (PND) 20 (PND 0: the day of delivery). On PND 2, four male and four female offspring per dam were randomly selected and remaining litters were culled. On PND 20, 20 male and 20 female offspring (at least one male and one female per dam) per group were subjected to prepubertal necropsy [16,18]. All animals were weighed and sacrificed by exsanguination from the abdominal aorta under deep anesthesia with ether. Animal protocols were reviewed and approved by the Animal Care and Use Committee of the National Institute of Health Sciences, Japan.

2.3. Preparation of tissue specimens and microdissection

For microarray and real-time reverse transcription (RT)-polymerase chain reaction (PCR) analyses, the whole brain of male offspring was immediately removed at prepubertal necropsy on PND 20 (n = 4/group) and fixed with methacarn solution for 2 h at 4 °C [10]. Coronal brain slices taken at −3.5 mm from the bregma were dehydrated and embedded in paraffin. Embedded tissues were stored at 4 °C until tissue sectioning for microdissection [19].

For microdissection, 4 and 20 μm-thick serial sections were prepared. The 4 μm-thick sections were stained with hematoxylin and eosin for confirmation of anatomical orientation of the hippocampal substructure to aid microdissection (Fig. 1). The 20 μm-thick sections were mounted onto PEN-foil film (Leica Microsystems GmbH, Welzlar, Germany) overlaid on glass slides, dried in an incubator overnight at 37 °C, and then stained using an LCM staining kit (Ambion, Inc., Austin, TX). Regions of CC and bilateral cerebral white matter (external capsule) in sections, as shown in Fig. 1, were subjected to laser microbeam microdissection (Leica Microsystems GmbH). Forty sections from each animal were used for microdissection, and microdissected samples were individually stored in 1.5 ml tubes at −80 °C until total RNA extraction.

2.4. RNA preparation, amplification and microarray analysis

Total RNA extraction from microdissected regions, quantitation of RNA yield, and RNA amplification were performed using methods described elsewhere [14,15,19].

For microarray analysis, second-round-amplified biotin-labeled antisense RNAs were subjected to hybridization with a GeneChip® Rat Genome 230 2.0 Array (Affymetrix, Inc., Santa Clara, CA).

Gene selection and normalization of expression data were performed using GeneSpring® software 7.2 (Silicon Genetics, Redwood City, CA). Per chip normalization was performed according to a method described elsewhere [14,15]. Genes with expression changes of at least 2-fold in magnitude compared with those of untreated controls were selected. Common genes with altered expression in anti-thyroid agent exposed groups were also selected.

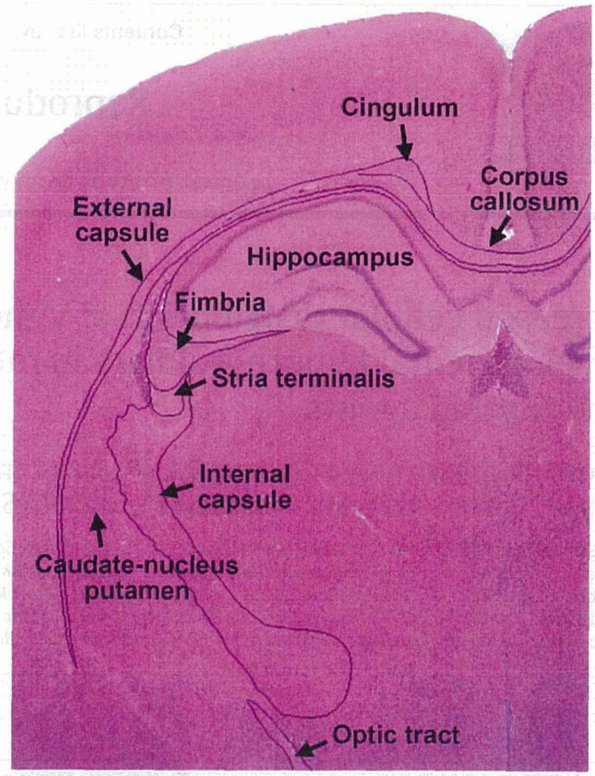

Fig. 1. Overview of the cerebral hemisphere of a male rat at PND 20 stained with hematoxylin and eosin. Magnification, 12.5×.

2.5. Real-time RT-PCR

Quantitative real-time RT-PCR using an ABI Prism 7900HT (Applied Biosystems Japan Ltd., Tokyo, Japan) was performed for confirmation of expression values obtained from microarray analysis. Selected genes showed altered expression (≥2-fold, ≤0.5-fold) in any of the anti-thyroid agent-exposed animals as compared with those of untreated controls. For example, vimentin, *Ret*, v-maf musculoaponeurotic fibrosarcoma oncogene (*v-Maf*) and tektin 4 as up-regulated genes, and *Cld11* and zinc finger homeobox 1b (*Zfhx1b*) as down-regulated ones. RT was performed using first-round antisense RNAs prepared for microarray analysis. For real-time PCR analysis, ABI Assays-on-Demand™ TaqMan® probe and primer sets from Applied Biosystems (n = 4/group) were used. For quantification of expression data, a standard curve method was applied. Expression values were normalized to glyceraldehyde 3-phosphate dehydrogenase (GAPDH) using TaqMan® Rodent GAPDH Control Reagents (Applied Biosystems Japan Ltd.).

2.6. Immunohistochemistry

To evaluate the immunohistochemical distribution of molecules identified by microarray analysis, the brains of male pups obtained at PND 20 were fixed in Bouin's solution at room temperature overnight. Ten animals for each group were used except for the untreated control group with six animals.

Antibodies against vimentin (mouse monoclonal antibody, 1:200; Millipore Corporation, Billerica, MA), glial fibrillary acidic protein (GFAP, rabbit polyclonal antibody, 1:500; Dako, Glostrup, Denmark), Ret (rabbit polyclonal antibody, 1:50; Santa Cruz Biotechnology, Inc., Santa Cruz, CA), DCC (mouse monoclonal antibody, 1:40; Leica Microsystems GmbH), and oligodendrocyte specific protein (OSP, same as Cld11, rabbit polyclonal antibody, 1:200; Novus Biologicals, Inc., Co., Littleton, CO) were used for immunohistochemistry. For antigen retrieval, sections were heated in 10 mM citrate buffer in a microwave for 10 min before incubation with anti-vimentin and -DCC antibodies. Immunodetection was carried out using a VECTASTAIN® Elite ABC kit (Vector Laboratories Inc., Burlingame, CA) with 3,3′-diaminobenzidine/H_2O_2 for the chromogen as described elsewhere [13,14]. Sections were then counterstained with hematoxylin and coverslipped for microscopic examination.

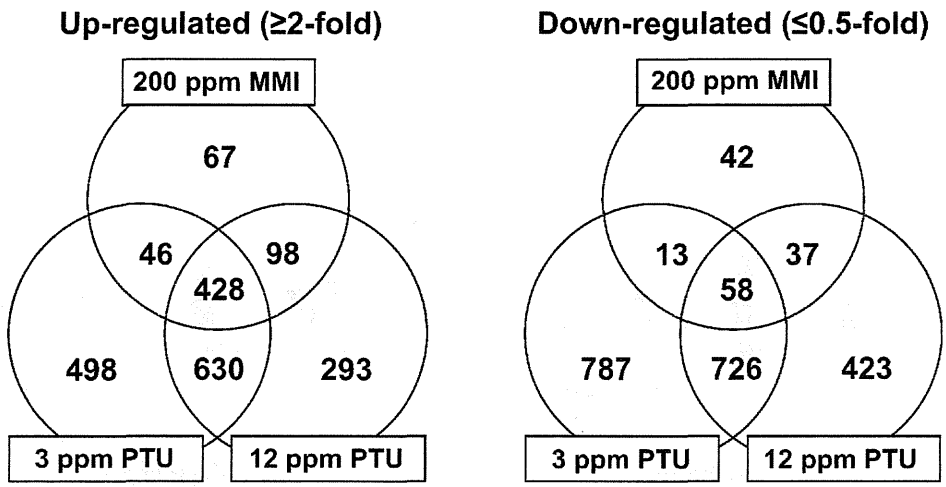

Fig. 2. Venn diagram of genes with altered expression in microarray analysis in response to maternal exposure to anti-thyroid agents. (Left) Up-regulated genes (≥2-fold). (Right) Down-regulated genes (≤0.5-fold).

2.7. Morphometry of immunolocalized cells

The number of immunoreactive cells was quantitatively measured by vimentin and Ret expression in white matter at the cingulum of the bilateral sides using two sections with an approximately 100 μm interval (i.e. four images per animal; Fig. 1), and values were normalized and expressed as those in the unit area (cm^2). GFAP-immunoreactive cells were similarly measured. For quantitative measurement of each immunoreactive cellular component containing vimentin, Ret and GFAP, digital photomicrographs at 100-fold magnification were taken using a BX51 microscope (Olympus Optical Co., Ltd., Tokyo, Japan) attached to a DP70 Digital Camera System (Olympus Optical Co.), and quantitative measurements were performed using WinROOF image analysis software 5.7 (Mitani Corp., Fukui, Japan). To evaluate immunoreactivity of DCC and Cld11 in white matter, staining intensity was scored as 0 (none), 1 (minimal), 2 (slight), 3 (moderate) and 4 (strong) by observation at 40-fold magnification.

2.8. Statistical analysis

Numerical data were assessed by one-way analysis of variance or the Kruskal–Wallis test following Bartlett's test. Statistically significant differences were analyzed by Dunnett's multiple test for comparison with that of the untreated control group. For grading immunohistochemical findings, scores of DCC and Cld11 expression were analyzed with the Mann-Whitney's *U*-test between the untreated control group and each anti-thyroid agent treated group.

3. Results

3.1. Global gene expression analysis

Fig. 2 shows the Venn diagram of genes with altered expression in microdissected cerebral white matter in treated groups in combination or individually in each treated group. Numerous common genes were found to be up- or down-regulated in two of the three treatment groups. The number of genes with up- or down-regulation in response to 3 ppm PTU was higher compared with that of 12 ppm PTU. The number of genes with

Table 1
List of representative genes associated with brain development showing up- or down-regulation common to treatments with MMI and PTU at both 3 and 12 ppm (≥2-fold, ≤0.5-fold).

Accession no.	Gene title	Symbol	MMI	PTU, 3 ppm	PTU, 12 ppm
Up-regulated (20 genes)					
NM_052803	ATPase, Cu++ transporting, alpha polypeptide	*Atp7a*	5.02	11.39	11.09
NM_001108322	T-box 1	*Tbx1*	4.20	4.34	2.31
NM_001191609	Laminin, alpha 5	*Lama5*	4.11	11.57	9.35
NM_031550	Cyclin-dependent kinase inhibitor 2A	*Cdkn2a*	3.59	2.70	3.37
NM_001114330	Glutamate receptor, metabotropic 1	*Grm1*	3.45	2.92	5.89
(NM_001114330)			(3.01)	(2.85)	(2.88)
NM_023091	gamma-Aminobutyric acid A receptor, epsilon	*Gabre*	3.20	3.91	7.46
NM_001107692	Ephrin A4	*Efna4*	3.13	5.07	6.72
NM_001002805	Complement component 4a	*C4a*	3.04	7.15	6.43
NM_019328	Nuclear receptor subfamily 4, group A, member 2	*Nr4a2*	2.97	2.87	4.92
NM_001110099	Ret proto-oncogene	*Ret*	2.89	5.01	4.39
NM_053629	Follistatin-like 3	*Fstl3*	2.85	4.28	6.08
NM_053708	Gastrulation brain homeobox 2	*Gbx2*	2.82	4.73	4.09
NM_019236	Hairy and enhancer of split 2	*Hes2*	2.76	2.93	3.11
NM_001109223	Wingless-related MMTV integration site 16	*Wnt16*	2.71	2.42	3.82
XM_001077495	Nuclear receptor co-repressor 1	*Ncor1*	2.67	2.01	2.97
NM_001012220	Cation channel, sperm associated 2	*Catsper2*	2.54	6.69	4.56
NM_001024275	Ras association (RalGDS/AF-6) domain family 4	*Rassf4*	2.31	4.67	5.43
NM_138900	Complement component 1, s subcomponent	*C1s*	2.12	3.31	3.88
NM_031140	Vimentin	*Vim*	2.11	6.01	4.27
NM_053555	Vesicle-associated membrane protein 5	*Vamp5*	2.04	2.62	3.41
Down-regulated (4 genes)					
NM_013107	Bone morphogenetic protein 6	*Bmp6*	0.23	0.38	0.25
NM_053759	Sine oculis homeobox homolog 1	*Six1*	0.45	0.35	0.46
NM_019280	Gap junction membrane channel protein alpha 5	*Gja5*	0.46	0.16	0.28
NM_133293	GATA binding protein 3	*Gata3*	0.47	0.47	0.24

Abbreviations: MMI, 2-mercapto-1-methylimidazole; PTU, 6-propyl-2-thiouracil.

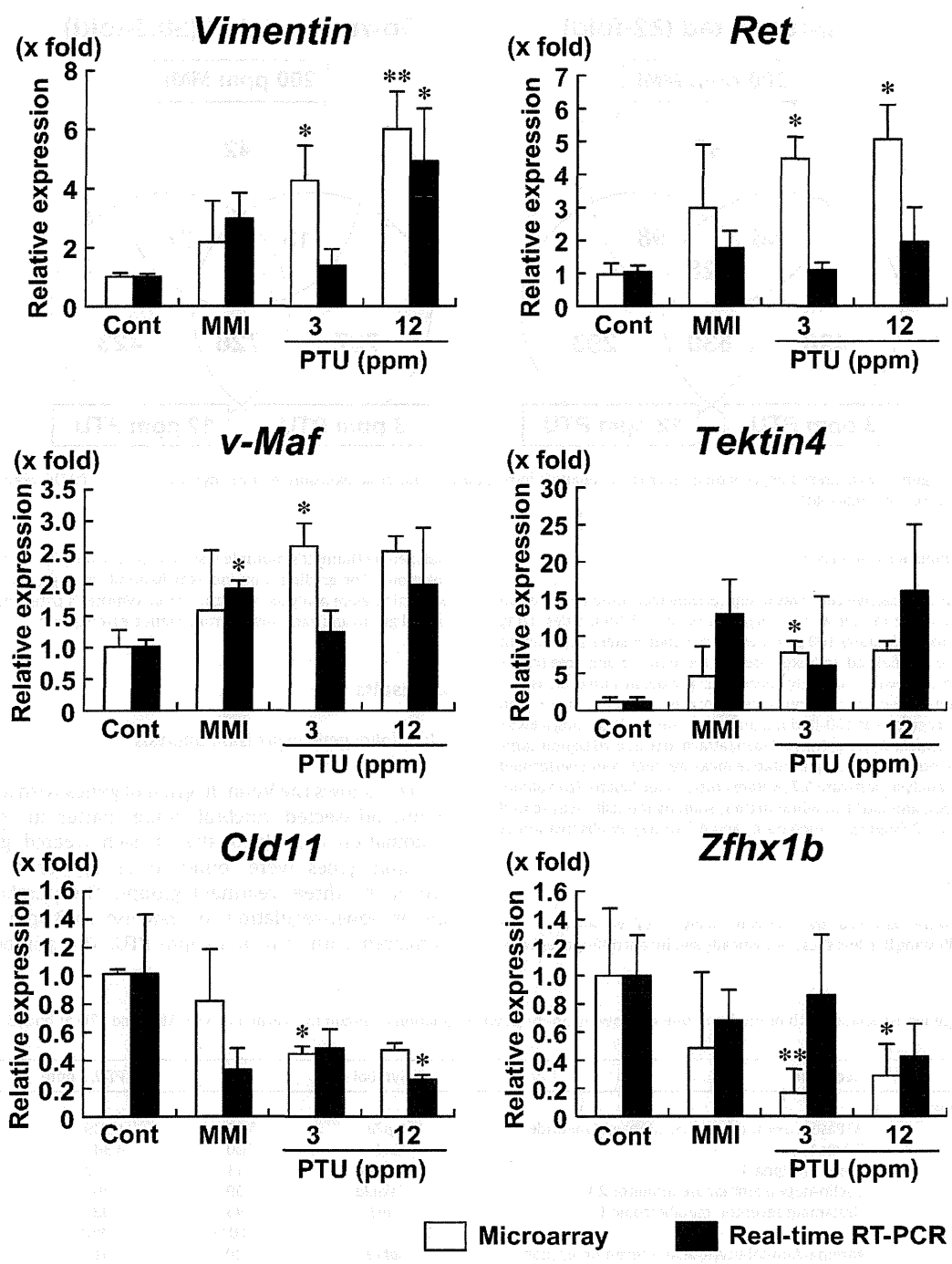

Fig. 3. Validation of mRNA expression of genes selected from microarray data ($n = 4$ in each group). *$P < 0.05$, **$P < 0.01$ vs. untreated controls.

up- or down-regulation in response to 200 ppm MMI was much lower compared with those of both PTU groups. Four hundred and eighty six common genes (428 up-regulated; 58 down-regulated) were identified with altered expression between MMI and both PTU groups (Fig. 2 and Supplementary data: Tables 1 and 2). Among these genes, the genes associated with central nervous system (CNS) development, cell differentiation and cell adhesion were commonly up- or down-regulated in response to anti-thyroid agents (Supplementary data: Tables 1 and 2). Twenty-four genes (20 up-regulated; 4 down-regulated) were related to CNS development involving glial cell differentiation, axon guidance, myelination, and cellular migration (Table 1). Among them, 12 up-regulated genes and two down-regulated genes showed PTU dose-dependent expression changes. For confirmation of microarray data, four genes that were up-regulated and two genes that were down-regulated in response to anti-thyroid agents were selected for mRNA expression analysis by real-time RT-PCR. Results are summarized in Fig. 3. All genes examined showed fluctuations in transcript levels in any of anti-thyroid agent treatment groups, which was similar to that of microarray data.

3.2. Immunolocalization of selected molecules in cerebral white matter

Immunohistochemical localization of vimentin, Ret, DCC and Cld11 was examined in the cerebral white matter. Within white

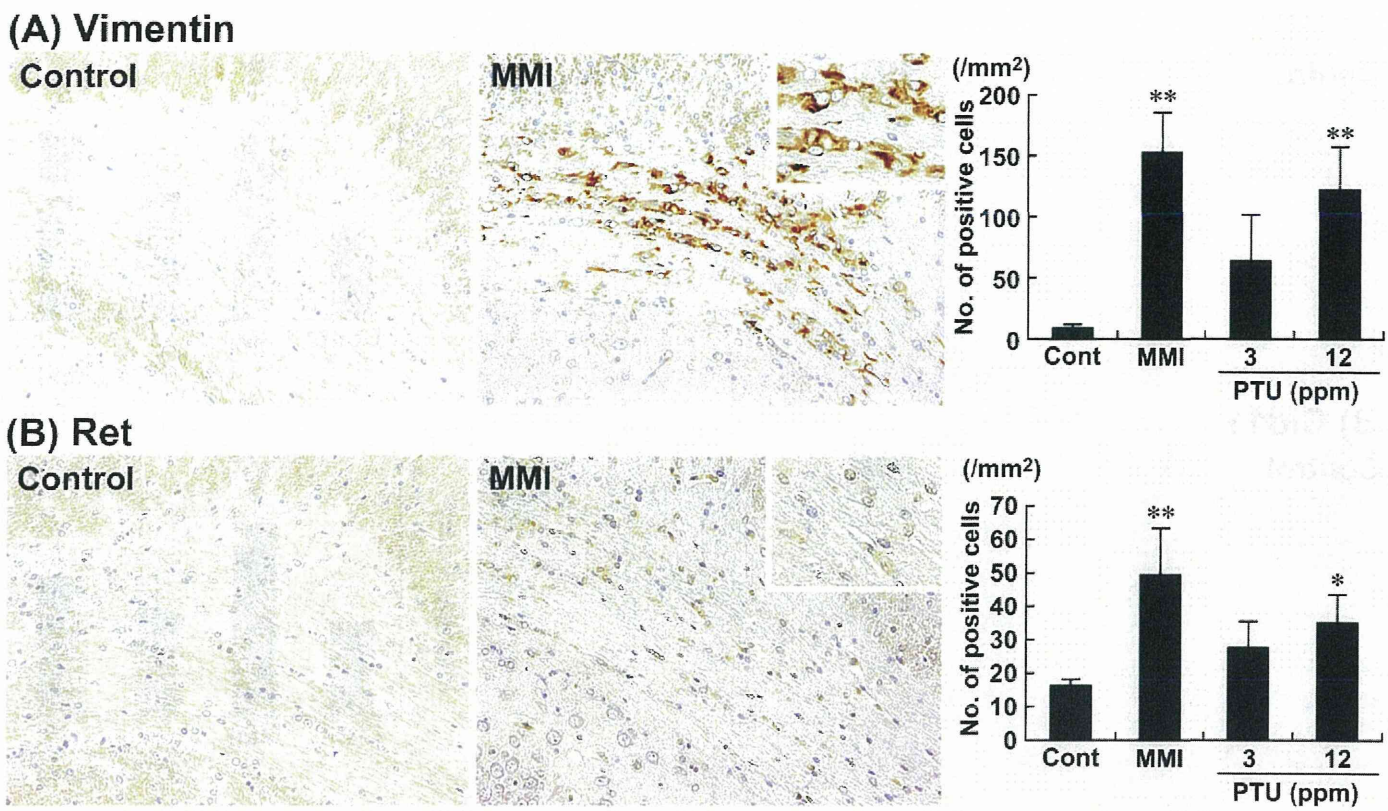

Fig. 4. Immunohistochemical distributions of vimentin- and Ret-positive cells in the while matter tissue. (A) Vimentin-immunoreactive cells in the cingulum. Untreated control animal (left) and MMI-treated animal (right). 200× magnification (inset: 400× magnification). Graph shows the mean number of positive cells within the cingulum at 200× magnification (untreated controls: $n=6$; MMI and PTU groups: $n=10$). $^{**}P<0.01$ vs. untreated controls. (B) Ret-immunoreactive cells in the cingulum. Untreated control animal (left), MMI-treated animal (right). 200× magnification (inset: 400× magnification). Graph shows the mean number of positive cells within the cingulum at 100× magnification (untreated controls: $n=6$; MMI and PTU groups: $n=10$). $^{*}P<0.05$, $^{**}P<0.01$ vs. untreated controls.

matter tissues, vimentin-immunoreactive cells were scarcely distributed in untreated control animals (Fig. 4A). After treatment with anti-thyroid agents, the distribution of vimentin-positive cells were mainly observed in the cingulum with a statistically significant increase in number with MMI and 12 ppm PTU treatments (Fig. 4A).

Ret-immunoreactive cells were mainly observed in white matter tissues of untreated control animals (Fig. 4B). After treatment with anti-thyroid agents, Ret-positive cells were mainly observed in the cingulum with a statistically significant increase in number with MMI and 12 ppm PTU treatments (Fig. 4B).

DCC showed diffuse immunoreactivity in white matter, indicating myelin sheaths with a statistically significant increase in the intensity scores of animals treated with MMI and 12 ppm PTU as compared with those of the untreated control (Fig. 5A).

Diffuse Cld11-immunoreactivity was observed in white matter, indicating myelin sheaths (Fig. 5B). The immunoreactivity showed a statistically significant increase in the intensity score of animals treated with MMI as compared with that of the untreated control (Fig. 5B).

3.3. Immunolocalization of GFAP

To investigate the cell type of vimentin-positive cells, cellular distribution of GFAP immunoreactivity was analyzed as a marker of astrocytes. Untreated control animals showed scattered distribution of GFAP-immunoreactive cells in cerebral white matter, and the number of GFAP-immunoreactive cells was higher compared with that of vimentin-positive cells. GFAP-immunoreactive cells showed a similar distribution to that of vimentin-immunoreactive cells, with accumulated distribution in the cingulum (Fig. 6). After treatment with anti-thyroid agents, the number of GFAP-positive cells was significantly increased in animals treated with MMI and 12 ppm PTU.

4. Discussion

In our previous study [16], maternal exposure to MMI and PTU induced typical hypothyroidism-related changes in the concentration of thyroid-related hormones, and variability in the distribution of hippocampal CA1 pyramidal neurons due to neuronal mismigration [16]. With regard to thyroid hormone-related changes in functions or structures in glial cell populations, gene expression alternations have been reported in myelin-related protein genes related to oligodendrocytes [20,21], as well as in enzymes or cytoskeletal components related to astrocytes [22–24]. Therefore, both oligodendrocytes and astrocytes could also be the target of developmental hypothyroidism. We, in the above-mentioned study [16], also observed changes in white matter structures with hypoplasia due to impaired oligodendroglial development as previously reported [2,9]. Using the same study samples, we, in the present study, analyzed immunohistochemical distribution of molecules that showed fluctuations in gene expression from microarray analysis of cerebral white matter tissue collected using microdissection targeting oligodendrocytes and astrocytes. This is the first report to use microarray analysis of gene expression changes induced by developmental hypothyroidism in white matter, whereas there have been such approaches for the study of cerebral cortex and hippocampal substructures [15,25,26]. We found that anti-thyroid agents caused fluctuations in a number of genes associated with CNS development involving glial cell differentiation, axon guidance, myelination, and cellular migration as listed in Table 1. Among them, vimentin, Ret, DCC and Cld11

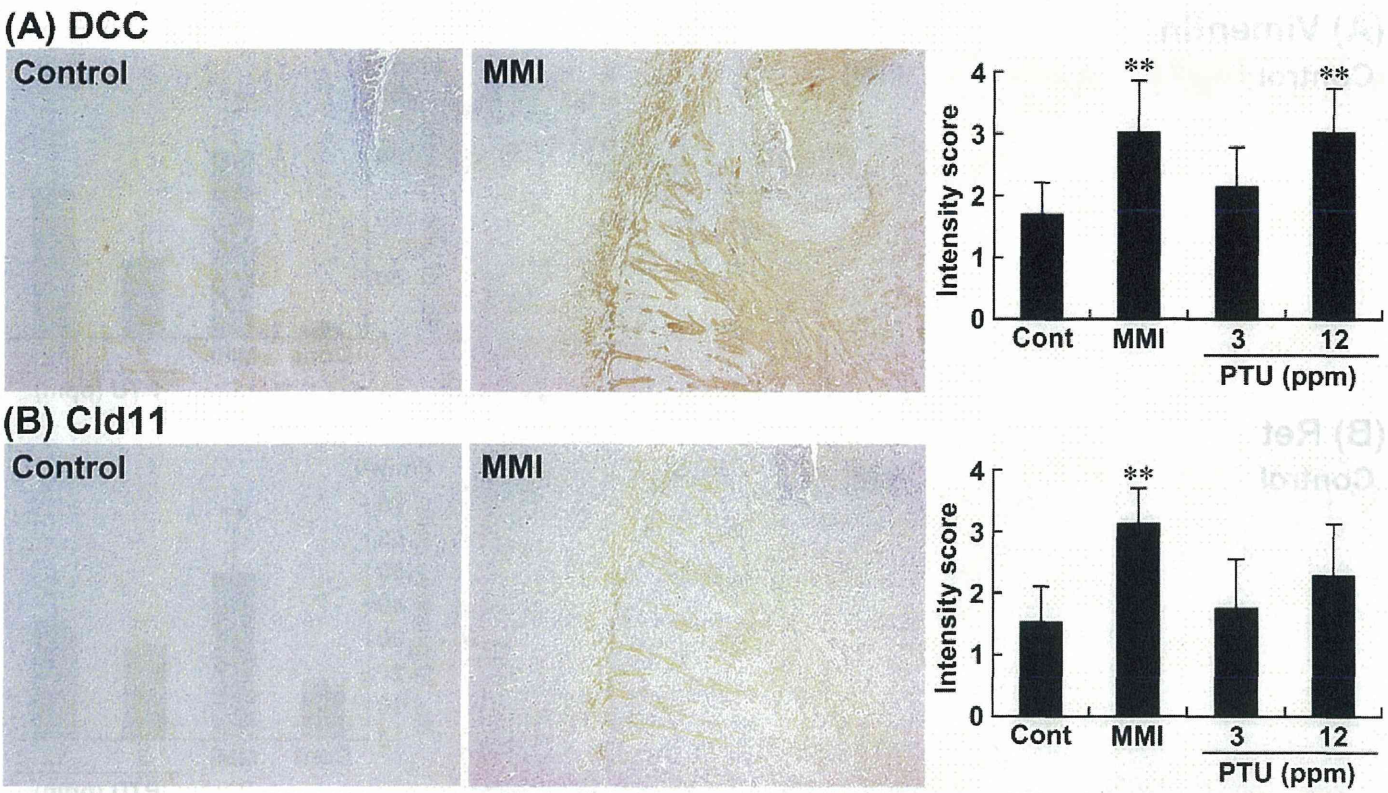

Fig. 5. Immunohistochemical distributions of DCC- and Cld11 in the while matter tissue. (A) DCC-immunoreactivity in the myelin sheath of the external capsule, internal capsule, and fimbria of the hippocampus. Untreated control animal (left), MMI-treated animal (right). 40× magnification. Graph shows the mean intensity score of immunoreactivity at 40× magnification (untreated controls: $n = 6$; MMI and PTU groups: $n = 10$). $^{**}P < 0.01$ vs. untreated controls. (B) Cld11-immunoreactivity in the myelin sheath of the external capsule, internal capsule, and fimbria of the hippocampus. Untreated control animal (left), MMI-treated animal (right). 40× magnification. Graph shows the mean intensity score of immunoreactivity at 40× magnification (untreated controls: $n = 6$; MMI and PTU groups: $n = 10$). $^{**}P < 0.01$ vs. untreated controls.

showed immunohistochemical distribution changes in the cerebral white matter of offspring after maternal exposure to PTU and MMI.

Cld11 is a four-transmembrane protein, which is primarily expressed in oligodendrocytes of the CNS and is the third most abundant CNS myelin protein [27–29]. Cld11 is involved in the formation of intramembranous tight junctions within the myelin sheath [30]. It is known that developmental hypothyroidism results in continued reduction of oligodendrocytes in the CC region from PND 10 [2]. In vitro study has shown that Cld11-overexpression results in induction of oligodendrocyte proliferation [31]. This result indicates that the overexpression of Cld11 at PND 20 is a compensatory response to decrease numbers of oligodendrocytes. However, mRNA levels were inconsistently decreased, suggesting involvement of post-transcriptional events such as those regulating mRNA stability and protein turnover.

DCC is a transmembrane receptor for netrin-1 via the fourth fibronectin type III domain [32]. Netrin-1 is a secreted protein, which elicits both attractive and repulsive responses in axonal guidance, neuronal migration and oligodendroglial migration depending on the homomeric or heteromeric combination of receptor dimers including DCC and Unc5 [33–35]. Netrin-1 signaling via DCC mediates growth cone extension and myelin sheath formation [36,37]. Therefore, increased expression of DCC in the myelin sheath at PND 20 induced by developmental hypothyroidism in the present study suggests a compensatory increase in response to suppression of myelin sheath formation [2]. However,

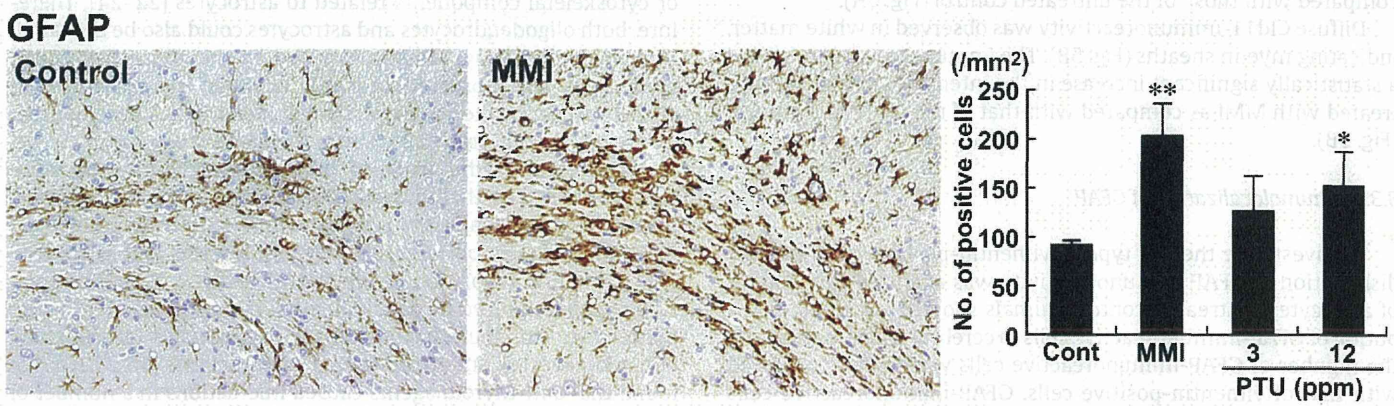

Fig. 6. Immunohistochemical distributions of GFAP-positive cells in the cingulum. Untreated control animal (left), MMI-treated animal (right). 200× magnification. Graph shows the mean number of positive cells within the cingulum at 200× magnification (untreated controls: $n = 6$; MMI and PTU groups: $n = 10$). $^{*}P < 0.05$, $^{**}P < 0.01$ vs. untreated controls.

DCC has an alternative function to drive cell death independent of both mitochondria-dependent and death receptor/caspase-8 pathways [38,39]. Moreover, DCC induces cell death in the absence of netrin-1 [40]. Because we did not find an increase in netrin-1 transcript levels using microarray analysis, it is possible that increased ligand-free DCC may lead to glial cell apoptosis. Progressive decrease in the CC area and the number of oligodendrocytes in this area during maturation after developmental hypothyroidism suggests the involvement of apoptosis due to increased ligand-free DCC [2,16].

Ret is a receptor protein–tyrosine kinase of glial cell line-derived neurotrophic factor (GDNF), a member of the transforming growth factor-β family [41]. GDNF signals play a critical role in development of the entire nervous system, kidney morphogenesis and spermatogenesis. While the functional relevance of Ret in oligodendrocytes has not been reported, this molecule is expressed in progenitor and immature oligodendrocytes in vitro and mediates cell proliferation induced by GDNF treatment [42]. Therefore, increased expression of Ret on PND 20 proceeding developmental hypothyroidism suggests a compensatory increase in response to decreased numbers of oligodendrocytes [2]. However, Ret induces cell death in the absence of its ligand similar to that of DCC [43]. Because we did not find an increase in GDNF transcript levels using microarray analysis, a progressive decrease in the size of the CC area and its oligodendrocyte density during maturation suggests involvement of apoptosis due to the increase of ligand-free Ret [2,16].

Vimentin is a member of the intermediate filament family of proteins. In the brain, this molecule is expressed in immature astrocytes during development [44–46]. Reactive astrocytes that are activated immature astrocytes during gliosis processes in response to injuries of CNS tissue also express vimentin [47,48]. Reactive astrocytes also express GFAP similar to that of mature astrocytes [47,48], suggesting that immature astrocytes can express both of vimentin and GFAP. On the other hand, developmental hypothyroidism leads to increase in vimentin expression in fetal rat brains [23]. Increase of GFAP-expression was also reported after developmental hypothyroidism in the CC region on PND 15 [49]. These results may suggest that developmental hypothyroidism increases the immature population of astrocytes. In the present study, vimentin-immunoreactive cells showed similar localization to those positive for GFAP. Therefore, a larger population of vimentin-positive cells in the cingulum induced by developmental hypothyroidism was considered to consist of immature astrocytes resembling reactive astrocytes. Interestingly, we previously reported frequent induction of subcortical band heterotopia in the CC, manifested by the appearance of aberrant cortical tissue in this anatomical area, in hypothyroid animals identical to the present study [16]. Anatomical location of this heterotopic tissue was close to the cingulum accumulating immature astrocytes, suggesting an etiological relation between the two. Alternatively, the increased immature astrocytes may simply be the reactive change in response to reduced oligodendrocytes due to developmental hypothyroidism [2,16,49]. However, developmental hypothyroidism may affect differentiation of neuronal progenitor cells, thereby inhibiting differentiation into oligodendrocytes, and instead, facilitating astrocytic differentiation during gliogenesis.

In conclusion, focusing on white matter development, we found aberrant expression of molecules associated with brain development after maternal exposure to anti-thyroid agents. Immunohistochemically, we found increased expression of Cld11, DCC, Ret and vimentin in white matter. Among them, vimentin and Ret were expressed in immature astrocytes and oligodendrocytes, respectively. Both positive cell populations were mainly distributed in the cingulum with the largest area of white matter. Because vimentin- and Ret-positive cells can be quantitatively evaluated, these molecules may be useful markers of glial cells, which respond to developmental exposure to thyroid hormone-disrupting chemicals.

Acknowledgments

We thank Tomomi Morikawa for her technical assistance in conducting the animal study. We also thank Ayako Kaneko for her technical assistance in preparing the histological specimens. This work was supported by Health and Labour Sciences Research Grants (Research on the Risk of Chemical Substances) from the Ministry of Health, Labour and Welfare of Japan. All authors disclose that there are no conflicts of interest that could inappropriately influence the outcome of the present study.

Appendix A. Supplementary data

Supplementary data associated with this article can be found, in the online version, at http://dx.doi.org/10.1016/j.reprotox.2012.03.005.

References

[1] Porterfield SP. Thyroidal dysfunction and environmental chemicals—potential impact on brain development. Environmental Health Perspectives 2000;108(Suppl. 3):433–8.
[2] Schoonover CM, Seibel MM, Jolson DM, Stack MJ, Rahman RJ, Jones SA, et al. Thyroid hormone regulates oligodendrocyte accumulation in developing rat brain white matter tracts. Endocrinology 2004;145:5013–20.
[3] Montero-Pedrazuela A, Venero C, Lavado-Autric R, Fernández-Lamo I, García-Verdugo JM, Bernal J, et al. Modulation of adult hippocampal neurogenesis by thyroid hormones: implications in depressive-like behavior. Molecular Psychiatry 2006;11:361–71.
[4] de Escobar GM, Obregón MJ, del Rey FE. Iodine deficiency and brain development in the first half of pregnancy. Public Health Nutrition 2007;10:1554–70.
[5] Comer CP, Norton S. Effects of perinatal methimazole exposure on a developmental test battery for neurobehavioral toxicity in rats. Toxicology and Applied Pharmacology 1982;63:133–41.
[6] Akaike M, Kato N, Ohno H, Kobayashi T. Hyperactivity and spatial maze learning impairment of adult rats with temporary neonatal hypothyroidism. Neurotoxicology and Teratology 1991;13:317–22.
[7] Guadaño Ferraz A, Escobar del Rey F, Morreale de Escobar G, Innocenti GM, Berbel P. The development of the anterior commissure in normal and hypothyroid rats. Brain Research Developmental Brain Research 1994;81:293–308.
[8] Lavado-Autric R, Ausó E, García-Velasco JV, Arufe Mdel C, Escobar del Rey F, Berbel P, et al. Early maternal hypothyroxinemia alters histogenesis and cerebral cortex cytoarchitecture of the progeny. Journal of Clinical Investigation 2003;111:954–7.
[9] Goodman JH, Gilbert ME. Modest thyroid hormone insufficiency during development induces a cellular malformation in the corpus callosum: a model of cortical dysplasia. Endocrinology 2007;148:2593–7.
[10] Shibutani M, Uneyama C, Miyazaki K, Toyoda K, Hirose M. Methacarn fixation: a novel tool for analysis of gene expressions in paraffin-embedded tissue specimens. Laboratory Investigation 2000;80:199–208.
[11] Uneyama C, Shibutani M, Masutomi N, Takagi H, Hirose M. Methacarn fixation for genomic DNA analysis in microdissected, paraffin-embedded tissue specimens. Journal of Histochemistry and Cytochemistry 2002;50:1237–45.
[12] Takagi H, Shibutani M, Kato N, Fujita H, Lee KY, Takigami S, et al. Microdissected region-specific gene expression analysis with methacarn-fixed, paraffin-embedded tissues by real-time RT-PCR. Journal of Histochemistry and Cytochemistry 2004;52:903–13.
[13] Shibutani M, Lee KY, Igarashi K, Woo GH, Inoue K, Nishimura T, et al. Hypothalamus region-specific global gene expression profiling in early stages of central endocrine disruption in rat neonates injected with estradiol benzoate or flutamide. Developmental Neurobiology 2007;67:253–69.
[14] Woo GH, Takahashi M, Inoue K, Fujimoto H, Igarashi K, Kanno J, et al. Cellular distributions of molecules with altered expression specific to thyroid proliferative lesions developing in a rat thyroid carcinogenesis model. Cancer Science 2009;100:617–25.
[15] Saegusa Y, Woo GH, Fujimoto H, Inoue K, Takahashi M, Hirose M, et al. Gene expression profiling and cellular distribution of molecules with altered expression in the hippocampal CA1 region after developmental exposure to anti-thyroid agents in rats. Journal of Veterinary Medical Science 2010;72:187–95.
[16] Shibutani M, Woo GH, Fujimoto H, Saegusa Y, Takahashi M, Inoue K, et al. Assessment of developmental effects of hypothyroidism in rats from in utero and lactation exposure to anti-thyroid agents. Reproductive Toxicology 2009;28:297–307.

[17] Masutomi N, Shibutani M, Takagi H, Uneyama C, Takahashi N, Hirose M. Impact of dietary exposure to methoxychlor, genistein, or diisononyl phthalate during the perinatal period on the development of the rat endocrine/reproductive systems in later life. Toxicology 2003;192:149–70.
[18] Nakamura R, Teshima R, Hachisuka A, Sato Y, Takagi K, Nakamura R, et al. Effects of developmental hypothyroidism induced by maternal administration of methimazole or propylthiouracil on the immune system of rats. International Immunopharmacology 2007;7:1630–8.
[19] Lee KY, Shibutani M, Inoue K, Kuroiwa K, U M, Woo GH, et al. Methacarn fixation—effects of tissue processing and storage conditions on detection of mRNAs and proteins in paraffin-embedded tissues. Analytical Biochemistry 2006;351:36–43.
[20] Ibarrola N, Rodríguez-Peña A. Hypothyroidism coordinately and transiently affects myelin protein gene expression in most rat brain regions during postnatal development. Brain Research 1997;752:285–93.
[21] Barradas PC, Vieira RS, De Freitas MS. Selective effect of hypothyroidism on expression of myelin markers during development. Journal of Neuroscience Research 2001;66:254–61.
[22] Farwell AP, Dubord-Tomasetti SA. Thyroid hormone regulates the expression of laminin in the developing rat cerebellum. Endocrinology 1999;140:4221–7.
[23] Evans IM, Pickard MR, Sinha AK, Leonard AJ, Sampson DC, Ekins RP. Influence of maternal hyperthyroidism in the rat on the expression of neuronal and astrocytic cytoskeletal proteins in fetal brain. Journal of Endocrinology 2002;175:597–604.
[24] Dasgupta A, Das S, Sarkar PK. Thyroid hormone promotes glutathione synthesis in astrocytes by up regulation of glutamate cysteine ligase through differential stimulation of its catalytic and modulator subunit mRNAs. Free Radical Biology and Medicine 2007;42:617–26.
[25] Royland JE, Parker JS, Gilbert ME. A genomic analysis of subclinical hypothyroidism in hippocampus and neocortex of the developing rat brain. Journal of Neuroendocrinology 2008;20:1319–38.
[26] Kobayashi K, Akune H, Sumida K, Saito K, Yoshioka T, Tsuji R. Perinatal exposure to PTU decreases expression of Arc, Homer 1, Egr 1 and Kcna 1 in the rat cerebral cortex and hippocampus. Brain Research 2009;1264:24–32.
[27] Bronstein JM, Popper P, Micevych PE, Farber DB. Isolation and characterization of a novel oligodendrocyte-specific protein. Neurology 1996;47:772–8.
[28] Bronstein JM, Micevych PE, Chen K. Oligodendrocyte-specific protein (OSP) is a major component of CNS myelin. Journal of Neuroscience Research 1997;50:713–20.
[29] Morita K, Sasaki H, Fujimoto K, Furuse M, Tsukita S. Claudin-11/OSP-based tight junctions of myelin sheaths in brain and Sertoli cells in testis. Journal of Cell Biology 1999;145:579–88.
[30] Gow A, Southwood CM, Li JS, Pariali M, Riordan GP, Brodie SE, et al. CNS myelin and sertoli cell tight junction strands are absent in Osp/claudin-11 null mice. Cell 1999;99:649–59.
[31] Tiwari-Woodruff SK, Buznikov AG, Vu TQ, Micevych PE, Chen K, Kornblum HI, et al. OSP/claudin-11 forms a complex with a novel member of the tetraspanin super family and beta1 integrin and regulates proliferation and migration of oligodendrocytes. Journal of Cell Biology 2001;153:295–305.
[32] Kruger RP, Lee J, Li W, Guan KL. Mapping netrin receptor binding reveals domains of Unc5 regulating its tyrosine phosphorylation. Journal of Neuroscience 2004;24:10826–34.
[33] Serafini T, Colamarino SA, Leonardo ED, Wang H, Beddington R, Skarnes WC, et al. Netrin-1 is required for commissural axon guidance in the developing vertebrate nervous system. Cell 1996;87:1001–14.
[34] Alcántara S, Ruiz M, De Castro F, Soriano E, Sotelo C. Netrin 1 acts as an attractive or as a repulsive cue for distinct migrating neurons during the development of the cerebellar system. Development 2000;127:1359–72.
[35] Spassky N, de Castro F, Le Bras B, Heydon K, Quéraud-LeSaux F, Bloch-Gallego E, et al. Directional guidance of oligodendroglial migration by class 3 semaphorins and netrin-1. Journal of Neuroscience 2002;22:5992–6004.
[36] Fazeli A, Dickinson SL, Hermiston ML, Tighe RV, Steen RG, Small CG, et al. Phenotype of mice lacking functional Deleted in colorectal cancer (Dcc) gene. Nature 1997;386:796–804.
[37] Rajasekharan S, Baker KA, Horn KE, Jarjour AA, Antel JP, Kennedy TE. Netrin 1 and Dcc regulate oligodendrocyte process branching and membrane extension via Fyn and RhoA. Development 2009;136:415–26.
[38] Forcet C, Ye X, Granger L, Corset V, Shin H, Bredesen DE, et al. The dependence receptor DCC (deleted in colorectal cancer) defines an alternative mechanism for caspase activation. Proceedings of the National Academy of Sciences of the United States of America 2001;98:3416–21.
[39] Furne C, Corset V, Hérincs Z, Cahuzac N, Hueber AO, Mehlen P. The dependence receptor DCC requires lipid raft localization for cell death signaling. Proceedings of the National Academy of Sciences of the United States of America 2006;103:4128–33.
[40] Mehlen P, Rabizadeh S, Snipas SJ, Assa-Munt N, Salvesen GS, Bredesen DE. The DCC gene product induces apoptosis by a mechanism requiring receptor proteolysis. Nature 1998;395:801–4.
[41] Sariola H, Saarma M. Novel functions and signalling pathways for GDNF. Journal of Cell Science 2003;116:3855–62.
[42] Strelau J, Unsicker K. GDNF family members and their receptors: expression and functions in two oligodendroglial cell lines representing distinct stages of oligodendroglial development. Glia 1999;26:291–301.
[43] Bordeaux MC, Forcet C, Granger L, Corset V, Bidaud C, Billaud M, et al. The RET proto-oncogene induces apoptosis: a novel mechanism for Hirschsprung disease. EMBO Journal 2000;19:4056–63.
[44] Pixley SK, de Vellis J. Transition between immature radial glia and mature astrocytes studied with a monoclonal antibody to vimentin. Brain Research 1984;317:201–9.
[45] Ciesielski-Treska J, Goetschy JF, Ulrich G, Aunis D. Acquisition of vimentin in astrocytes cultured from postnatal rat brain. Journal of Neurocytology 1988;17:79–86.
[46] Alonso G. Proliferation of progenitor cells in the adult rat brain correlates with the presence of vimentin-expressing astrocytes. Glia 2001;34:253–66.
[47] Pekny M, Wilhelmsson U, Bogestål YR, Pekna M. The role of astrocytes and complement system in neural plasticity. International Review of Neurobiology 2007;82:95–111.
[48] Eddleston M, Mucke L. Molecular profile of reactive astrocytes—implications for their role in neurologic disease. Neuroscience 1993;54:15–36.
[49] Sharlin DS, Bansal R, Zoeller RT. Polychlorinated biphenyls exert selective effects on cellular composition of white matter in a manner inconsistent with thyroid hormone insufficiency. Endocrinology 2006;147:846–58.

The Journal of Toxicological Sciences (J. Toxicol. Sci.)
Vol.37, No.2, 373-380, 2012

Original Article

Development of humanized steroid and xenobiotic receptor mouse by homologous knock-in of the human steroid and xenobiotic receptor ligand binding domain sequence

Katsuhide Igarashi[1], Satoshi Kitajima[1], Ken-ichi Aisaki[1], Kentaro Tanemura[1], Yuhji Taquahashi[1], Noriko Moriyama[1], Eriko Ikeno[1], Nae Matsuda[1], Yumiko Saga[2,3], Bruce Blumberg[4] and Jun Kanno[1]

[1]Division of Cellular and Molecular Toxicology, Biological Safety Research Center, National Institute of Health Sciences, 1-18-1 Kamiyoga, Setagaya-ku, Tokyo, 158-8501, Japan
[2]Division of Mammalian Development, National Institute of Genetics, Yata 1111, Mishima 411-8540, Japan
[3]The Graduate University for Advanced Studies (Sokendai), Yata 1111, Mishima 411-8540, Japan
[4]Department of Developmental and Cell Biology, 2011 Biological Sciences 3, University of California, Irvine, CA 92697-2300, USA

(Received December 7, 2011; Accepted January 12, 2012)

ABSTRACT — The human steroid and xenobiotic receptor (SXR), (also known as pregnane X receptor PXR, and NR1I2) is a low affinity sensor that responds to a variety of endobiotic, nutritional and xenobiotic ligands. SXR activates transcription of Cytochrome P450, family 3, subfamily A (CYP3A) and other important metabolic enzymes to up-regulate catabolic pathways mediating xenobiotic elimination. One key feature that demarcates SXR from other nuclear receptors is that the human and rodent orthologues exhibit different ligand preference for a subset of toxicologically important chemicals. This difference leads to a profound problem for rodent studies to predict toxicity in humans. The objective of this study is to generate a new humanized mouse line, which responds systemically to human-specific ligands in order to better predict systemic toxicity in humans. For this purpose, the ligand binding domain (LBD) of the human SXR was homologously knocked-in to the murine gene replacing the endogenous LBD. The LBD-humanized chimeric gene was expressed in all ten organs examined, including liver, small intestine, stomach, kidney and lung in a pattern similar to the endogenous gene expressed in the wild-type (WT) mouse. Quantitative reverse transcription-polymerase chain reaction (RT-PCR) analysis showed that the human-selective ligand, rifampicin induced Cyp3a11 and Carboxylesterase 6 (Ces6) mRNA expression in liver and intestine, whereas the murine-selective ligand, pregnenolone-16-carbonitrile did not. This new humanized mouse line should provide a useful tool for assessing whole body toxicity, whether acute, chronic or developmental, induced by human selective ligands themselves and subsequently generated metabolites that can trigger further toxic responses mediated secondarily by other receptors distributed body-wide.

Key words: Steroid and xenobiotic receptor, Pregnane X receptor, Humanized mouse, Ligand binding domain, Knock-in mouse

INTRODUCTION

Most orally administered xenobiotics are metabolized first by the intestine and then by the liver after portal transport. The expression levels of enzymes involved in xenobiotic metabolism are regulated at the transcriptional level by key xenobiotic sensors including the steroid and xenobiotic receptor (SXR), also known as the pregnane X receptor (PXR), pregnane activated receptor (PAR) and NR1I2 (Bertilsson *et al.*, 1998; Lehmann *et al.*, 1998; Blumberg *et al.*, 1998). SXR is important in the field of toxicology for at least two reasons. Firstly, this receptor system induces the expression of CYP3A and CYP2B enzymes, the major metabolizers of pharmaceu-

Correspondence: Jun Kanno (E-mail: kanno@nihs.go.jp)

ticals and xenobiotics. Therefore, SXR is a key mediator of drug- and chemical-induced toxicity as well as drug-drug and drug-nutrient interactions (Zhou *et al.*, 2004). Secondly, the orthologous rodent and human receptors exhibit differential sensitivity for a subset of chemical ligands important in the field of toxicology. For example, rifampicin (RIF) is a specific and selective activator of human SXR, whereas pregnenolone 16a-carbonitrile (PCN) is selective for the rodent orthologue.

Rodent-human differences in CYP3A and CYP2B-mediated responses to xenobiotics can be a profound problem in toxicologic studies where rodents are used to predict the toxicity of a compound in humans (Ma *et al.*, 2007). Therefore, development of a murine model that reconstructs the SXR-mediated systemic response of humans is of a great significance in toxicology.

Human and rodent SXRs share ~95% amino acid sequence identity in the DNA-binding domain (DBD) but only about 77% identity in the LBD. Tirona *et al.* (2004) analyzed the ligand selectivity of a human-rat chimeric protein and showed that the species differences are primarily defined by sequence differences in the LBD. Watkins and colleagues showed that the key residues responsible for the majority of the ligand selectivity were Leu 308 (human) and Phe305 (rat and mouse). Crystallographic analysis located these amino acids within or neighboring the flexible loop that forms a part of the pore to the ligand-binding cavity. Swapping the rodent and human-specific residues was shown to modulate the activation by the human-selective activator RIF *in vitro* (Watkins *et al.*, 2001). According to those findings, a simple replacement of the mouse LBD with the human sequence should be sufficient to "humanize" the ligand binding properties as well as activation of the downstream target genes.

Three kinds of humanized mice have already been generated. One is the SXR-null/Alb-SXR mouse (Alb-SXR mouse) made by crossing the SXR knockout mice with a transgenic mouse line that expresses human SXR in liver under the control of the albumin promoter (Xie *et al.*, 2000). Gonzalez and colleagues generated a transgenic mouse expressing a human BAC containing the entire hSXR gene in a SXR null background, thus controlled under human SXR promoter (SXR BAC mouse) (Ma *et al.*, 2007). Another mouse is the human SXR genome knock-in mice (hSXR genome mouse) (Scheer *et al.*, 2008). The human SXR genomic region from exon 2 to exon 9 was knocked-in to mouse SXR exon 2. This mouse expresses the human full length SXR mRNA under the control of mouse SXR promoter regulation. Although useful for toxicology studies, these mice have disadvantages in that the human SXR is expressed only in the liver (Alb-SXR mouse), hSXR mRNA is not expressed in all of the tissues where SXR is known to be expressed (SXR BAC mouse), and there might be potential differences in the binding affinities of hSXR DNA-binding domain (DBD) to *cis*-acting elements in mouse SXR target genes (hSXR genome mouse).

As noted above, it is known that the critical differences between human and rodent ligand-selectivity reside in the LBD. Therefore, when our project to generate a humanized SXR mouse was initiated, we reasoned that altering the LBD would be sufficient to generate a humanized ligand selectivity. We decided to retain the mouse DBD to avoid any potential differences between the binding affinities of the chimeric receptor for cis-acting elements in the mouse genome. To maintain the tissue-specific expression pattern of the endogenous gene, we inserted the human cDNA encoding the region carboxyl-terminal to the DBD into the mouse gene. This retains all of the 5' and 3' regulatory elements in the mouse gene, as well as introns 1 and 2, which contain important elements for regulating SXR expression (Jung *et al.*, 2006).

Here we report a new line of mouse (hSXRki mouse) in which a cDNA encoding the human LBD is homologously recombined into the mouse gene after exon 3. The tissue distribution of the resulting chimeric mouse DBD-human LBD mRNA is comparable to that of the WT mouse. The hSXRki mouse showed a fully humanized response to the human-selective activator RIF in that the Cyp3a11 mRNA was induced in liver and mucosa of small intestine in response to RIF, but not the rodent-selective compound PCN. This new mouse line should provide a useful tool for assessing the whole body toxicity induced by a human selective SXR ligand itself and its subsequently generated metabolite(s) that can trigger further toxic responses through other pathways body-wide.

MATERIALS AND METHODS

Generation of hSXRki knock-in mice

A DNA fragment of mouse SXR intron 2 to exon 3 was PCR amplified using mouse BAC DNA (BAC clone No. RP23-351P21) as a template. Primers used were BAC39486FW and mSXR462RV (for sequences of the primers see Table1). This fragment was connected to the LBD of human SXR cDNA from amino acid 105 through the carboxyl terminus amplified by the PCR primers: hSXR904FW and hSXR1887RVEcoRI (template; human SXR cDNA). The 3'UTR of bovine growth hormone (BGH) was added to 3' to the terminal codon. This concatenated fragment was introduced to a vector, which

Table 1. List of primer pairs

Purpose	Primer name	Sequence (5' to 3')
Targeting vector construction	BAC39486FW	CCATGGGTACCACGAATAACAA
	mSXR462RV	CATGCCACTCTCCAGGCA
	hSXR904FW	AAGAAGGAGATGATCATGTCCG
	hSXR1887RVEcoRI	CCGAATTCTCATCATCAGCTACCTGTGATACCGAACA
Genotyping	NeoAL2	GGGGATGCGGTGGGCTCTATGGCTT
	SXR RC RV5	TGAGAGTGCACAAGTTCAAGCT
	WTInt5	AGTGATGGGAACCACTCCTG
	WTEx6RV	TGGTCCTCAATAGGCAGGTC
	mhSXRE4	GTGAACGGACAGGGACTCAG
	mhSXRSARV	CTCTCCTGGCTCATCCTCAC
Percellome quantitative RT-PCR	Cyp3a11 FW	CAGCTTGGTGCTCCTCTACC
	Cyp3a11 RV	TCAAACAACCCCCATGTTTT
	Ces6 FW	GGAGCCTGAGTTCAGGACAGAC
	Ces6 RV	ACCCTCACTGTTGGGGTTC
	mouse SXR FW	AATCATGAAAGACAGGGTTC
	mouse SXR RV	AAGAGCACAGATCTTTCCG
	human SXR FW	ATCACCCGGAAGACACGAC
	human SXR RV	AAGAGCACAGATCTTTCCG
	mouse-human SXR FW	CCCATCAACGTAGAGGAGGA

has the neomycin resistance gene with loxP sequence at both ends, removable with Cre recombinase (Saga *et al.*, 1999). A 7kb KpnI fragment containing intron 2 was used as a long arm and 1.3kb PstI-EcoRI fragment containing from exon 8 to intron 8 was used as a short arm for homologous recombination (Fig. 1). The resulting targeting vector was linearized with SacII and introduced by electroporation to TT2 ES cell line (Yagi *et al.*, 1993) and neomycin resistant clones were selected, PCR genotyped, and confirmed by the Southern blotting. For generation of chimeric mice, these ES clones were aggregated with ICR 8-cell embryos and transferred to pseudopregnant female recipients. The chimeric mice born were bred with ICR females. Germ line transmission of the targeted allele was confirmed by PCR. A mouse was crossed with a CAG-Cre transgenic mouse (Sakai and Miyazaki, 1997) to evict the neomycin resistance gene, and back crossed to C57BL/6 CrSlc (SLC, Inc., Shizuoka, Japan) at least 6 generations and used for the analysis.

PCR Genotyping (See Table 1 for primer sequences)

Primers for identification of homologously recombined ES clones were NeoAL2 and SXR RC RV5. DNA purified from the tail of each mouse was used for PCR genotying. Primers for WT detection were WTInt5 and WTEx6RV amplifying a product of 755 bp. Primers for confirmation of removal of the neomycin resistance gene were mhSXRE4 and mhSXRSARV amplifying a product of 1,223 bp.

Southern blot analysis

To confirm homologous recombination, DNA from ES cell cultures was purified and digested with BamHI and XhoI, then electrophoresed and analyzed by Southern hybridization (Saga *et al.*, 1997). Mouse SXR exon 9 region which remains after homologous recombination was used for the probe. The restriction fragments from the WT allele and targeted allele are 2,305 bp and 1,925 bp, respectively.

Chemicals

RIF (molecular weight 822.95) and PCN (molecular weight 341.49) were purchased from Sigma-Aldrich (St. Louis, MO, USA). Corn oil was purchased from Wako Pure Chemical Industries (Osaka, Japan).

Quantitative RT-PCR (Percellome PCR) (See Table 1 for primer sequences)

The method for Percellome quantitative RT-PCR was described previously (Kanno *et al.*, 2006). Briefly, tissue pieces stored in RNAlater (Ambion, Austin, TX, USA) were homogenized and lysed in RLT buffer (Qiagen GmbH., Germany) and 10 μl aliquots were used

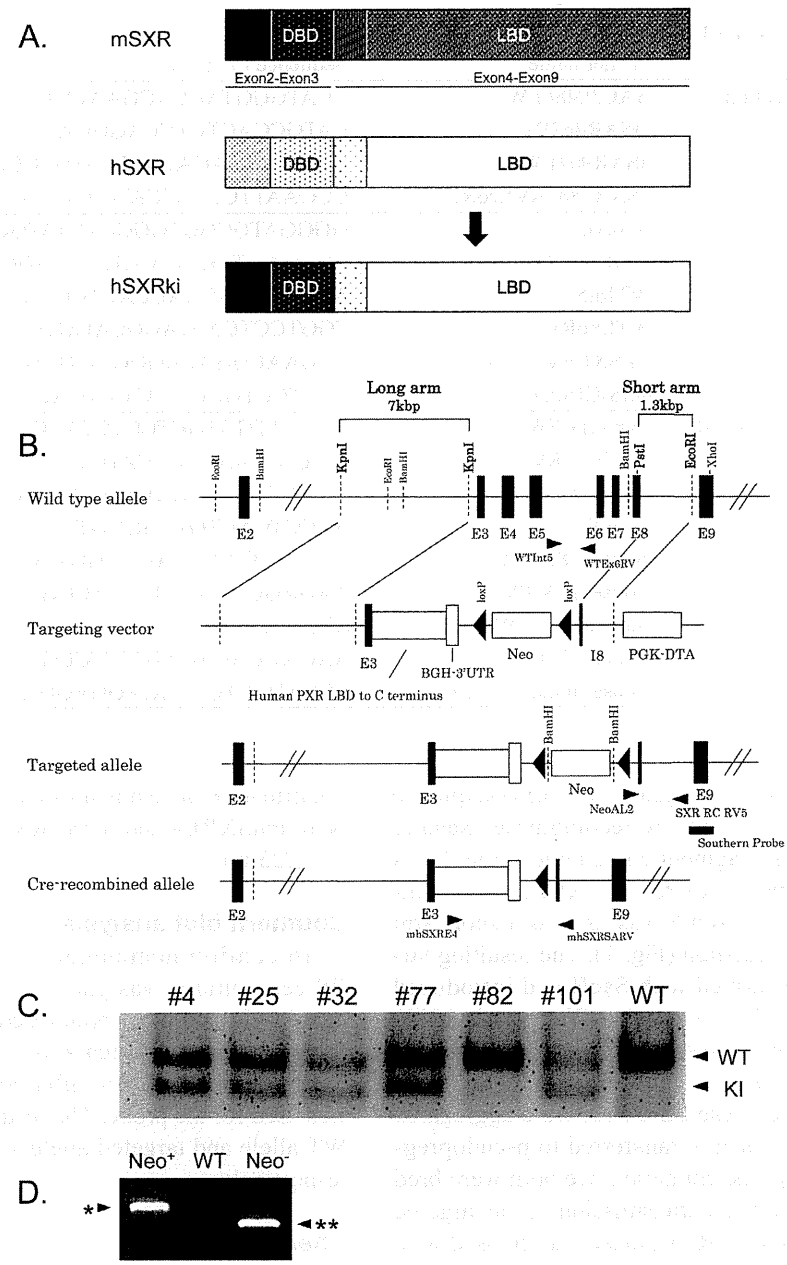

Fig. 1. Targeting strategy used to generate the hSXRki mouse. A) Diagram of hSXRki chimeric protein. Hinge region and ligand binding domain (LBD) of human SXR are knocked-in to mouse SXR, resulting in chimeric protein having murine N-ternial domain and DNA binding domain (DBD). B) Targeting strategy used to generate the hSXRki mouse. The chimeric mouse DBD and human LBD fragment, followed by the BGH 3' UTR were knocked-in to the mouse SXR gene. The genomic region spanning from exon 3 to exon 8 was substituted by the inserted fragment with the remainder of the gene remaining intact. C) Confirmation of homologous recombination by southern blot analysis. Six ES clones positive for recombination by PCR genotyping were further analyzed by southern blot (clones #4 ~ #101). Lower bands (1925 bp) indicate successful homologous recombination; upper bands (2305 bp) correspond to WT allele. Clones #4, #25, #32, #77 and #101 were confirmed as homologous recombinants; clones #4 and #25 were used for the generation of chimeric mice. D) Confirmation of Cre-mediated removal of the neomycin resistance gene. Mouse tail genome DNA was PCR amplified with the primer set, mhSXRE4 and mhSXRSARV. *: 2,858 bp (for the mice having the neomycin resistance gene), **: 1,223 bp (for the mice without the neomycin resistance gene).

for genomic DNA quantification with PicoGreen fluorescent dye (Invitrogen, Carlsbad, CA, USA). A prepared spike mRNA cocktail solution containing known quantity of five mRNAs of bacillus subtilis was added to the tissue lysate in proportion to the DNA quantity. Total RNA was purified from the lysate using the RNeasy kit (Qiagen). One microgram of total RNA was reverse-transcribed with SuperScript II (Invitrogen). Quantitative real time PCR was performed with an ABI PRISM 7900 HT sequence detection system (Applied Biosystems) using SYBR Green PCR Master Mix (Applied Biosystems), with initial denaturation at 95°C for 10 min followed by 40 cycles of 30 sec at 95°C and 30 sec at 60°C and 30 sec at 72°C, and Ct values were obtained. Primers for Cyp3a11 were Cyp3a11 FW and Cyp3a11 RV. Primers for Ces6 were Ces6 FW and Ces6 RV. Primers for mouse SXR selective quantification were mouse SXR FW and mouse SXR RV. Primers for hSXRki selective quantification were human SXR FW and human SXR RV. Primers for both mouse SXR and hSXRki quantification were mouse-human SXR FW and mouse-human SXR RV that amplify the DBD region of the chimera.

In Situ Hybridization analysis

Digoxigein-labeled cRNA probe for Cyp3a11 was synthesized according to Suzuki *et al.* (2005) by RT-PCR using mouse liver cDNA as a template. The primers used were as follows: forward 5'-GATTGGTTTTGATGCCTGGT-3' and reverse 5'-CAAGAGCTCACATTTTTCATCA-3'. The amplified product was sequence confirmed and ligated with Block-iT T7-TOPO (Invitrogen) Linker, which contains the T7 promoter site. A secondary PCR was performed to generate the sense and antisense DNA templates. For antisense template, Block-iT T7 Primer and Cyp3a11 forward primer (or reverse primer for generation of sense DNA template), the same primer as for the first PCR amplification, were used. With these DNA templates, both sense and antisense digoxigenin-labeled riboprobes were synthesized using a DIG RNA labeling kit (Roche Diagnostics, Germany) according to the manufacturer's protocol.

ISH on paraffin sections was carried out according to Suzuki *et al.* with a modification; permeabilization condition 98°C for 15 min in HistoVT One (Nacalai tesque, Japan).

Animals experiments

Male hSXRki and WT mice were maintained under a 12 hr light/12 hr dark cycle with water and chow (CRF-1, Oriental Yeast Co. Ltd., Tokyo, Japan) provided *ad libitum*. The animal studies were conducted in accordance with the Guidance for Animal Studies of the National Institute of Health Sciences under Institutional approval. The expression level of the hSXRki and WT SXR mRNA of ten organs (brain, thymus, heart, lung, liver, stomach, spleen, kidney, small intestine and testis) were analyzed on 15 weeks old male mice (n = 2) by the Percellome quantitative RT-PCR.

For the demonstration of selective gene induction by RIF and PCN in hSXRki and WT male mice on 13 weeks

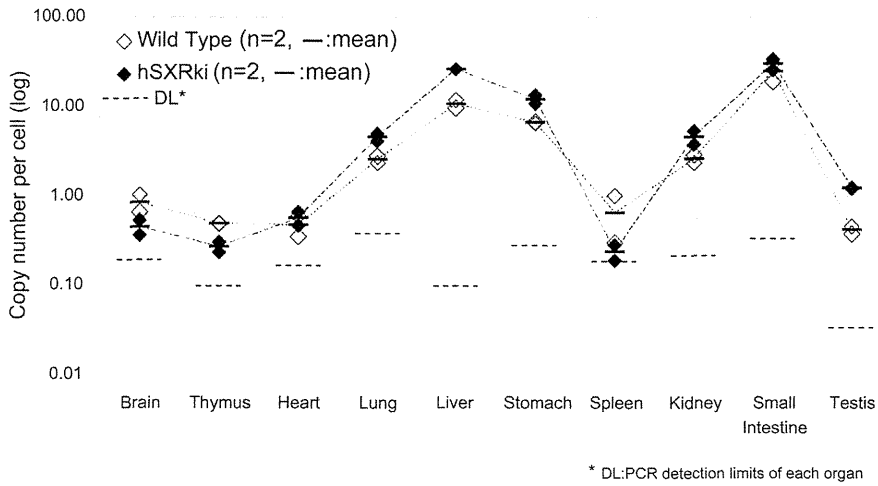

Fig. 2. Conservation of tissue expression patterns of hSXRki mRNA in the knock-in mouse. Percellome quantitative RT-PCR analysis was performed to measure the absolute expression levels of WT SXR mRNA and hSXRki mRNA in ten organs of WT and hSXRki mice. The expression levels of hSXRki mRNA among organs were comparable to WT.

old, three mice per group were singly dosed orally with vehicle (corn oil+0.1% DMSO), 10, 30, or 100 mg/kg of RIF, or 20, 70, or 200 mg/kg PCN (approximately equivalent in molar dose). Eight hours later, mice were sacrificed by exsanguination under ether anesthesia and the liver and the small intestine mucosa were sampled. Liver samples in small pieces were stored in RNA later (Applied Biosystems, Foster City, CA, USA) for further analysis. The small intestine under ice-cooled condition was longitudinally opened, gently rinsed with RNase-free saline and the epithelium was scraped with a glass slide and immersed in RNAlater. For *in situ* hybridization (ISH) of Cyp3a11 in the liver, 15 weeks old male hSXRki and WT mice were dosed orally with vehicle (corn oil), RIF (10 mg/kg), or PCN (40 mg/kg) daily for 3 days and liver sampled 24 hr later. All mice were sacrificed by exsanguination under ether anesthesia.

Statistical analysis

All values are expressed as the means ± S.D. and group differences analyzed by unpaired Student's *t* test or one-way ANOVA followed by Dunnett's post hoc comparison. Level of significance was set at $p < 0.05$.

RESULTS

Generation of hSXRki knock-In mice

Among 144 neomycin resistant TT2 ES clones, six PCR positive clones were further submitted to Southern blotting for the confirmation of homologous recombination. As shown in Fig. 1C, five clones were confirmed, and two (#4 and #25) were used to generate chimeric mice. The resulting mice were backcrossed to ICR strain to confirm germline transmission. One clone (#4) was crossed to a mouse constitutively expressing Cre recombinase to remove the neomycin resistance gene (Fig. 1D) and backcrossed to C57BL/6 CrSlc for at least 6 generations before further analysis.

Tissue distribution of hSXRki mRNA

Ten tissues, i.e., brain, thymus, heart, lung, liver, stomach, spleen, kidney, small intestine and testis from both hSXRki and WT mice were measured for hSXRki or WT SXR mRNA expression by the Percellome quantitative RT-PCR. As shown in Fig. 2, the levels of hSXRki mRNA are comparable to that of SXR in WT mouse and expressed in all tissues analyzed.

Humanized responses in hSXRki mouse

Humanized response of hSXRki was demonstrated by administration of the mouse-specific ligand PCN and the

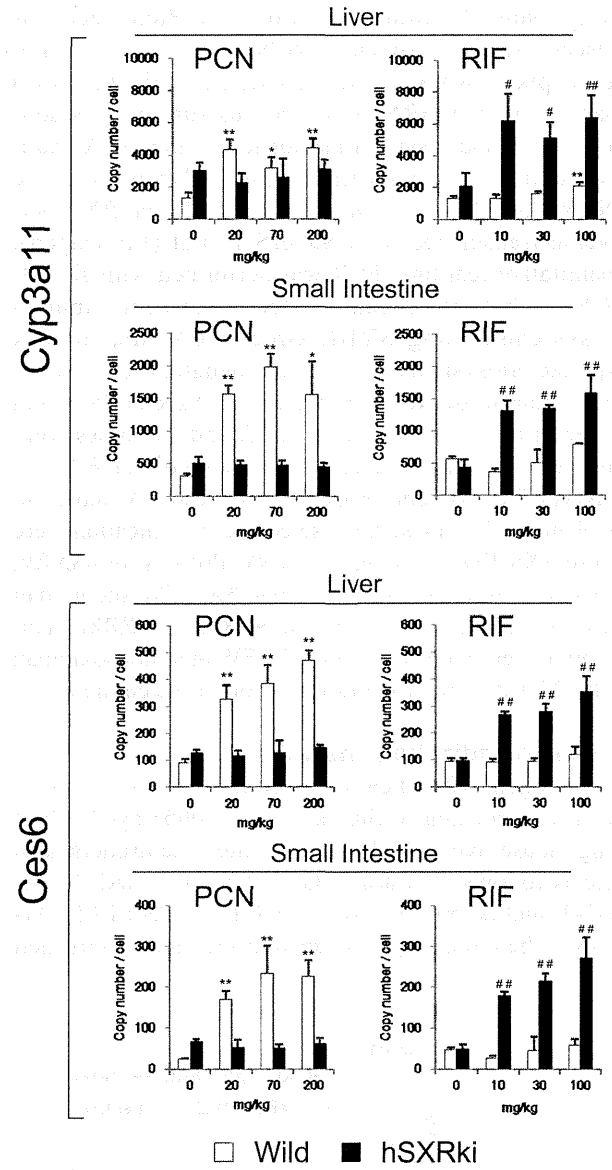

Fig. 3. Humanized response of hSXRki mice to RIF and PCN; Percellome quantitative RT-PCR. WT mice and hSXRki mice (n = 3 each) were singly dosed orally with vehicle (corn oil+0.1% DMSO), 20, 70, or 200 mg/kg PCN, or 10, 30, or 100 mg/kg of RIF (approximately equivalent in molar dose each other). Percellome quantitative RT-PCR data of Cyp3a11 and Ces6, both known as SXR target genes, in liver and small intestinal mucosa showed humanized responses in hSXRki. Bars = S.D., *; $p < 0.05$, **; $p < 0.01$ compared with vehicle group of WT, #; $p < 0.05$, ##; $p < 0.01$ compared with vehicle group of hSXRki. Analyzed by one-way ANOVA followed by Dunnett's post hoc comparison. Level of significance was set at $p < 0.05$.